Angewandte Chemie
Eine Zeitschrift der Gesellschaft Deutscher Chemiker

Supporting Information

Boosting Cycling Stability and Rate Capability of Li–CO_2 Batteries via Synergistic Photoelectric Effect and Plasmonic Interaction

K. Zhang, J. Li, W. Zhai, C. Li, Z. Zhu, X. Kang, M. Liao, L. Ye, T. Kong, C. Wang, Y. Zhao, P. Chen, Y. Gao, B. Wang, H. Peng**

Table of Contents

Experimental Procedures

Materials. Titanium wire (Ti, 99.7% metal basis, diameter: 0.25 mm) was purchased from Alfa Aesar. Acetone (99.5%), isopropanol (99.5%), methanol (99%), ethylene glycol butyl ether (99%), and ethylene glycol (99.5%) were obtained from Sinopharm Chemical Reagent Co., Ltd. Perchloric acid (assay, 70.0~72.0%) was purchased from Shanghai Titan Scientific Co., Ltd. Ammonium fluoride (NH_4F, ≥ 99.0% metals basis) was purchased from Shanghai Aladdin Biochemical Technology Co., Ltd. Lithium tablets (99.9%, thickness: 0.40 mm, diameter: 16 mm) were obtained from China Energy Lithium Co., Ltd. Bis(trifluoromethane)sulfonimide (LiTFSI, 99.95% trace metals basis), 1-ethyl-3-methylimidazolium tetrafluoroborate ($EMIMBF_4$, $C_6H_{11}BF_4N_2$, for electrochemistry, ≥ 99.0% HPLC), trimethylolpropane ethoxylate triacrylate (TMPET, molecular weight of ~428), 2-hydroxy-2-methyl-1-phenyl-1-propanone (HMPP, 97%), poly(vinylidene fluoride-co-hexafluoropropylene) (PVDF-HFP, average Mn of ~130000), 1,3-dioxolane (anhydrous, 99.8%), and silver nitrate (≥ 99.0%) were purchased from Sigma-Aldrich. N-methyl pyrrolidone (99.9%) was purchased from Aladdin Reagent. Glass fiber separator (GF/A,1.6 μm) was purchased from Whatman Co. Ltd. The CR2032-type stainless-steel coin cells with a hole (diameter: 12 mm) were purchased from Shenzhen Kelude Company.

Preparation of TiO_2 nanotube arrays (TNAs) cathodes. First, Ti wire (length: 5.0 cm, diameter: 200 μm) was washed with acetone, isopropanol, and deionized water in turn and dried at 70 °C in a vacuum drying oven. Then, it was put into a mixture of 42 wt% methanol, 53 wt% ethylene glycol butyl ether, and 5 wt% perchloric acid at 0 °C for a two-step electrochemical polishing. The first step was conducted at a constant voltage (35 V) for 15 s and the second step was at a constant voltage (20 V) for 20 s. The polished Ti wire was then rinsed thoroughly with deionized water and dried in a vacuum drying oven. Next, the polished Ti wire was used as the anode for anodization with a Pt foil as the counter electrode. The anodization was conducted in ethylene glycol electrolyte containing 0.3 wt% ammonium fluoride and 2 wt% deionized water for 45 min at a constant voltage (40 V) and temperature (40 °C). The anodized Ti wire was washed with deionized water and annealed in ambient air at 500 °C for 1 h with a heating rate of 8 °C·min^{-1} to obtain anatase TiO_2 nanotube arrays on the Ti wire.

Preparation of TiO_2 nanotube arrays @ Ag nanoparticles (TNAs@AgNPs) cathodes. Ag nanoparticles were deposited on the annealed TNAs by the galvanostatic method on an electrochemical workstation with TNAs as a working electrode and a Pt foil as the counter electrode. The galvanostatic method was carried out at 5 mA·cm^{-2} for 4 s in an aqueous solution containing 0.075 mM silver nitrate at room temperature. The obtained TNAs@AgNPs cathode was washed with deionized water and dried in the air. The sizes of TiO_2 nanotube arrays and the deposition amount of Ag nanoparticles were controlled by varying the experimental parameters (*e.g.*, operation time, voltage, and electrolyte composition) for anodization and electrodeposition.

Preparation of gel electrolyte. Both electrolyte preparation and battery assembly were conducted in an argon-filled glove box with O_2 and moisture contents below 1.0 ppm. First, a precursor solution of gel electrolyte was obtained by mixing 33 wt% solution A (1 M LITFSI in $EMIMBF_4$), 42 wt% solution B (20 wt% PVDF-HFP in N-methyl pyrrolidone), and 25 wt% solution C (0.34 wt% HMPP in TMPET). Typically, 1.313 g solution A, 1.667 g solution B, and 1.0 g solution C were needed for assembling 8 C2032 coin cells. Then, the well-mixed precursor solution was cast on a piece of glass fiber separator, followed by a 365 nm UV irradiation for about 10 s to obtain the milky white quasi-solid-state gel electrolyte. Here, a piece of glass fiber separator was utilized to avoid the short circuit of the battery.

Battery assembly and characterizations. The battery was assembled by successively stacking a lithium tablet anode, a gel electrolyte, and a TNAs or TNAs@AgNPs cathode (length: 15 mm, diameter: 200 μm) in a CR2032 coin cell with a hole (diameter: 12 mm) at the cathode. The current density and areal capacity were normalized based on the projected area of the effective light-receiving part of the fiber electrode ($S = 12 \times 10^{-1} \times 200 \times 10^{-4} = 0.024$ cm^2). A piece of colorless transparent polymethylpentene film was wrapped on the cathode hole to prevent the moisture. The assembled battery was rapidly transferred to a homemade glass testing bottle filled with CO_2 at a flow rate of 25 sccm (99.99%, Shanghai Tomoe Gases Co., Ltd). All measurements were started after a 3 h open-circuit step on the LAND cyclers (CT2001A, Wuhan LAND Ltd.). A 400 W Ultraviolet lamp (Shanghai Libi Vacuum Technology Co., Ltd.) was used as the light source in the electrochemical and photoelectrochemical measurements. The light power density was around 46.4 mW·cm^{-2} (CEL-NP2000, Beijing China Education Au-light Technology Co., Ltd.).

Analytical sample preparation. To characterize the discharged/recharged cathodes, the batteries were discharged/recharged with a cut-off capacity of 0.1 mAh·cm^{-2} at 0.1 mA·cm^{-2} under illumination or in dark, and then transferred into an argon glove box to extract the cathodes. The cathodes were immersed in 1,3-dioxolane to wash off the residual electrolytes, evaporated for drying, and stored in the glove box before measurements.

Characterizations. All the following measurements were carried out on the sides of electrodes facing illumination. The morphology and structure of cathodes were characterized by field-emission scanning electron microscopy (FESEM, Zeiss ultra-55, operated at 5 kV, all samples sputter-coated with a thin gold film, 20 Pa 5 mA for 60 s), transmission electron microscopy (TEM, Tecnai G2 F20 S-Twin), and X-ray diffraction (recorded on Bruker AXS D8 powder X-ray diffractometer with Cu Kα radiation in the 2θ range from 10° to 80°). Raman spectra were collected on the Horiba XploRA with 532 nm laser excitation wavelength. X-ray photoelectron spectroscopy measurements were performed on a Thermo Scientific K-Alpha with C 1s peak at 284.8 eV as a reference). Fourier transform infrared spectroscopy measurements were carried out on a Thermofisher Nicolet 6700 equipped with a diamond attenuated total reflectance accessory. The ultraviolet-visible diffusion reflectance measurements were operated on an ultraviolet-visible spectrophotometer (Perkin-Elmer Lambda 750).

Photoelectrochemical measurements. A 400 W Ultraviolet lamp (Shanghai Libi Vacuum Technology Co., Ltd) was used as the light source in the photoelectrochemical and electrochemical measurements. Mott-Schottky measurements, photocurrent response measurements, and electrochemical impedance spectra were carried out in the electrochemical workstation (CHI660E, Shanghai Chenhua Ltd.). In a quartz cell, the TNAs or TNAs@AgNPs, Pt foil, and saturated calomel electrode were used as the working electrode, counter electrode, and reference electrode, respectively, with 1 M Na_2SO_4 aqueous solution as electrolyte.

Energy band calculations. The band gaps were calculated *via* the Tauc plots,

$$\alpha h\nu = B(h\nu - E_g)^m \quad (1)$$

Where α is the molar absorption coefficient, h is Planck constant ($h = 4.13566769 \times 10^{-15}$ eV·s), v is the incident photon frequency, B is the proportionality constant, E_g is the optical bandgap of the semiconductor material, and m is related to the semiconductor material

and the type of transition. The Tauc plots were drawn with hv as the X-axis and $(\alpha hv)^{1/m}$ as the Y-axis, and the intersection of the linear part and the X-axis was the bandgap.

The band structure of semiconductor materials can be calculated by Mott-Schottky measurements based on Impedance-Potential electrochemical technique, with the initial and final potential around the open-circuit voltage and frequency (1000 Hz). The test provided potential, Z_r (real part of impedance), and Z_i (imaginary part of impedance). C_s (series capacity) can be obtained based on the following equation (2), where w is the angular frequency (w = 2 × π × frequency).

$$C_s=1/(w * Z_i) \quad (2)$$

The Mott-Schottky plots can be drawn with potential as the X-axis and $1/(C_s * C_s)$ as the Y-axis, while the flat-band potential E_{FB} is obtained by extrapolating the x intercept of the corresponding line. The conduction band (CB) and valence band (VB) energy levels can be calculated by the following equations.

$$E_{CB}(\text{V vs. SCE}) = E_{FB}(\text{V vs. SCE}) - 0.1 \quad (3)$$

$$E_{CB}(\text{V vs. RHE}) = E_{CB}(\text{V vs. SCE}) + 0.0591 * \text{pH} + 0.24 \quad (4)$$

$$E_{CB}(\text{V vs. } Li^+/Li) = E_{CB}(\text{V vs. RHE}) + 3.03 \quad (5)$$

$$E_{VB}(\text{V vs. } Li^+/Li) = E_{CB}(\text{V vs. } Li^+/Li) + E_g/e \quad (6)$$

Finite difference time domain simulations. The finite difference time domain is a numerical scheme to solve Maxwell's equation in space and time. This is done by discretizing them using a central difference quotient to replace the first-order partial derivative of the field quantity concerning time and space, and the field distribution can be obtained by recursively simulating the wave propagation process in the time domain. The simulations were performed by the FDTD solutions (Lumerical).[1] To predict the enhancement of electric near-field amplitude around TNAs@AgNPs and TNAs cathodes, we calculated in a representative geometry of the device. According to the experimental results, Ag nanoparticles with a diameter of 80 nm were positioned at the top surface of TiO_2 nanotubes with an inner diameter of 70 nm. The refractive indices of the materials were taken from the literature. In the propagation direction (z) we assumed the perfectly matched layer to truncate the computational domain. In the two transversal directions (x and y) periodic boundary conditions were chosen. The space was discretized with a resolution of 1 nm until the temporal evolution was simulated until the steady state was observed.

Density functional theory calculation methods. First-principles calculations were carried out using density functional theory (DFT) with generalized gradient approximation (GGA) of Perdew-Burke-Ernzerhof (PBE) implemented in the Vienna Ab-Initio Simulation Package (VASP).[2] The valence electronic states were expanded on the basis of plane waves with the core-valence interaction represented using the projector augmented plane wave (PAW) [3] approach and a cutoff of 400 eV. The Brillouin zone integration was sampled with 1 × 1 × 1 K-point meshes for geometry optimization. The structures were fully relaxed until the maximal force on each atom became less than 0.05 eV/Å. The anatase (101) surface was mimicked using a slab model containing 8 atomic layer which was separated by a vacuum layer of 1.8 nm. A 3 × 2 supercell was used to eliminate the interaction of adsorbed species and their images. A silver cluster containing four silver atoms was chosen to mimic the effects of silver nanoparticles. According to the intensity value of the Ultraviolet curing lamp in the experiment, the applied electric field component for computation could be calculated by the following equations.

$$Z_0 = \mu_0 c \quad (7)$$

$$H_0 = \sqrt{2S/Z_0} \quad (8)$$

$$E_0 = \sqrt{2Z_0 S} \quad (9)$$

Where Z_0 is the impedance of free space, μ_0 is the permeability of vacuum ($\mu_0 = 4\pi \times 10^{-7}$ H/m), c is the light speed ($c = 3 \times 10^8$ m/s), S is the electromagnetic wave intensity ($S = 42\ \text{mW/cm}^2$, the intensity of Ultraviolet lamp), H_0 is the magnetic field intensity, and E_0 is the electric field intensity. The incident electric field component was calculated to be 563 V/m. To facilitate the subsequent calculation process, the electric field intensity applied in the computation was 600 V/m.

The adsorption energy of gas phase molecule is calculated as equation (10):

$$\Delta E_{ad} = E_{substrate+molecule} - E_{substrate} - E_{molecule} \quad (10)$$

where $E_{substrate+molecule}$, $E_{substrate}$, and $E_{molecule}$ are the total energies of the whole system, the substrate, and the gas phase molecule, respectively.

Results and Discussions

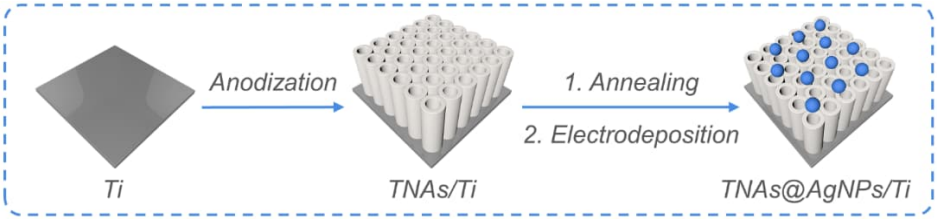

Figure S1. Preparation process of TNAs@AgNPs.

The geometrical parameters of TNAs and Ag nanoparticles could be adjusted by changing the operating time of anodization and electrodeposition, repectively. The resulting TNAs were selected to ensure large surface and abundant space for CO_2/ion transfer and product hosting, while the size and loading density of Ag nanoparticles were optimized to achieve the sufficient scattering and local intensified electric field for inhibited recombination.

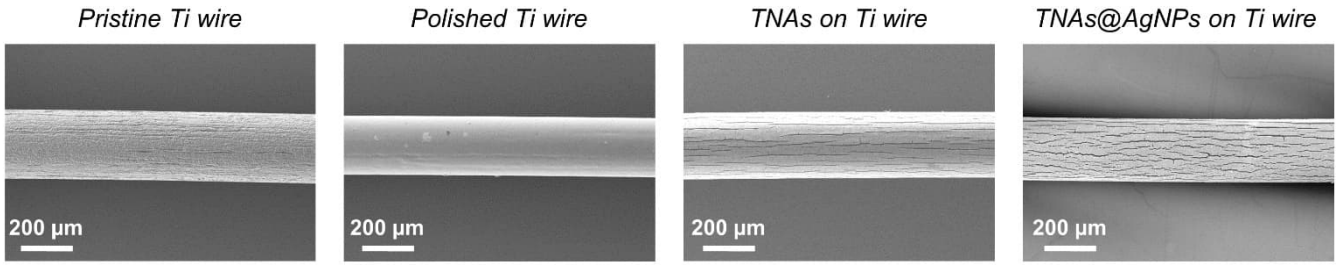

Figure S2. Scanning electron microscopy images of fiber electrodes.

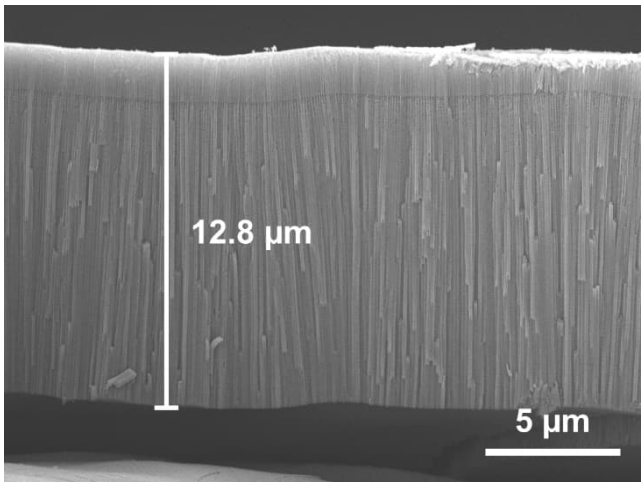

Figure S3. Scanning electron microscopy image of TNAs (side view).

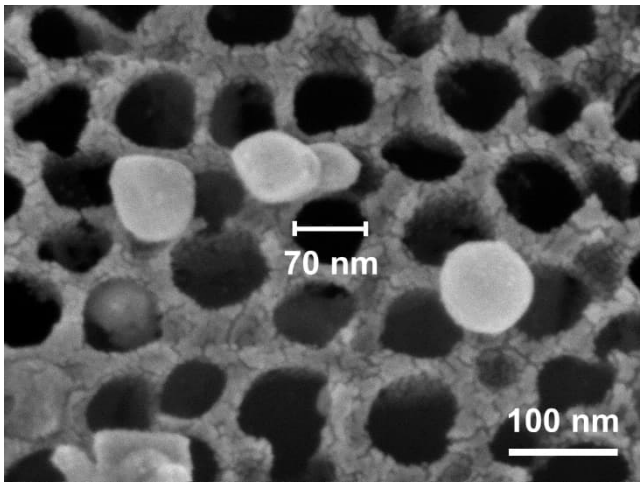

Figure S4. Scanning electron microscopy image of Ag nanoparticles on the TNAs (top view).

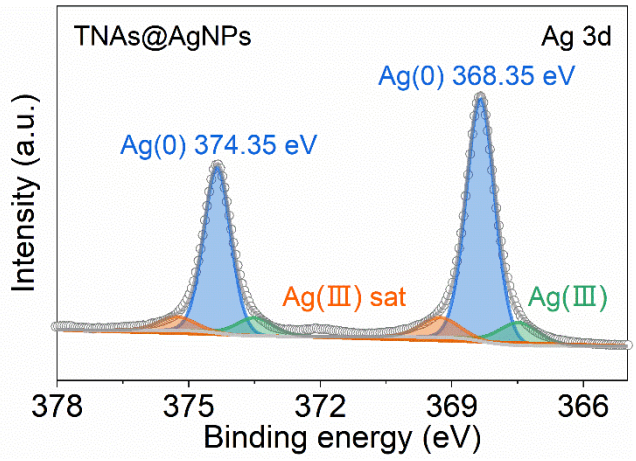

Figure S5. High-resolution Ag 3d X-ray photoelectron spectrum of TNAs@AgNPs.

The peaks at 368.35 eV and 374.35 eV in the Ag 3d X-ray photoelectron spectrum of TNAs@AgNPs were correlated with $3d_{5/2}$ and $3d_{3/2}$ of Ag (0), suggesting that Ag nanoparticles were not oxidized by air or TiO_2.

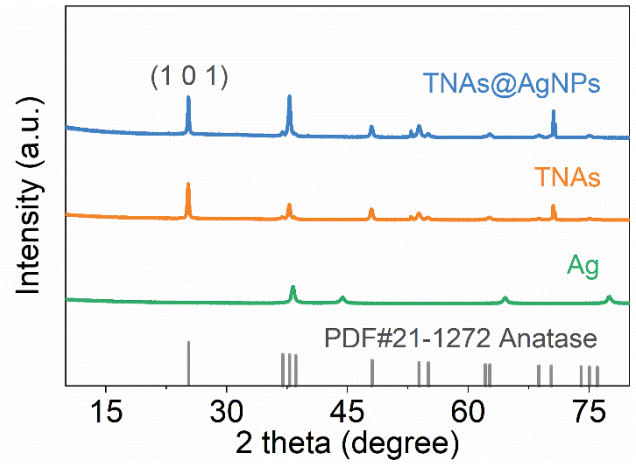

Figure S6. X-ray diffraction patterns of TNAs and TNAs@AgNPs.

The synthesized TNAs were confirmed as anatase crystal, and the indistinct signal of Ag in the TNAs@AgNPs was ascribed to its low content.

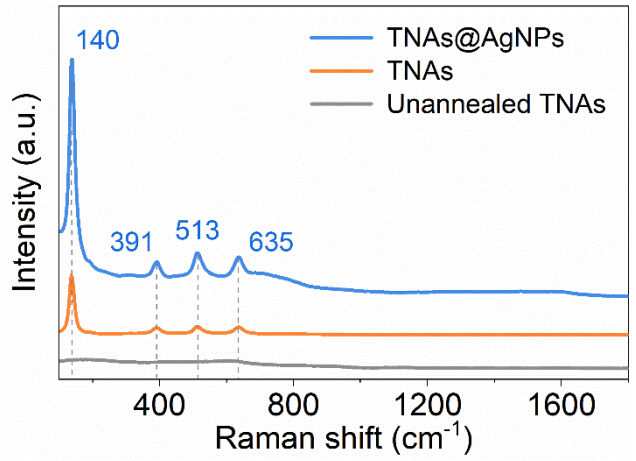

Figure S7. Raman spectra of unannealed TNAs, annealed TNAs, and TNAs@AgNPs.

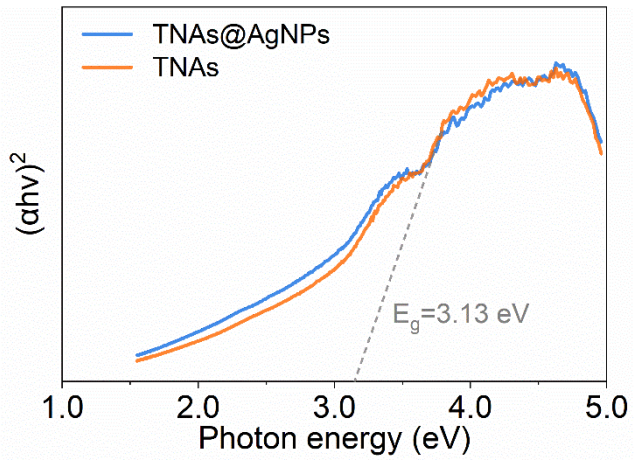

Figure S8. Tauc plots of TNAs and TNAs@AgNPs.

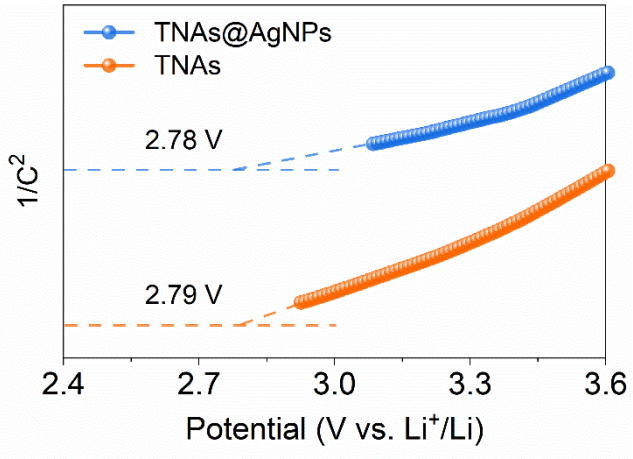

Figure S9. Mott-Schottky plots of TNAs and TNAs@AgNPs.

The E_{FB} values of TNAs and TNAs@AgNPs were estimated to be 2.79 V and 2.78 V vs. Li^+/Li, respectively. Therefore, the E_{CB} potentials were 2.69 and 2.68 V vs. Li^+/Li, respectively.

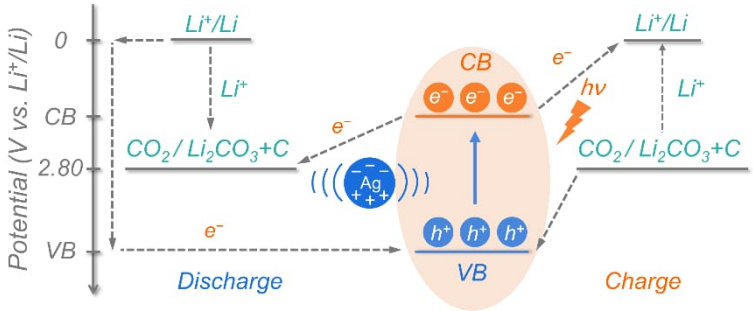

Figure S10. Reaction mechanism of the dual-field assisted Li-CO_2 battery based on TNAs@AgNPs cathode with illumination.

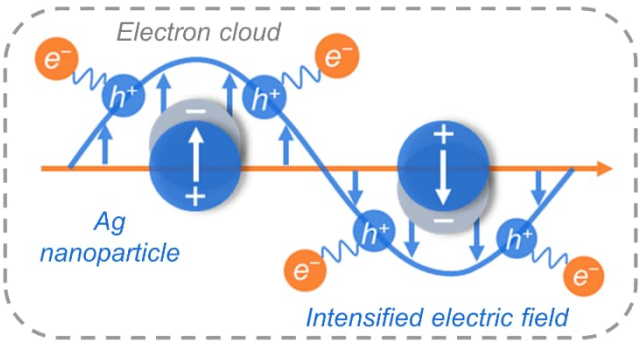

Figure S11. Fundamental principle and effect of local intensified electric field around Ag nanoparticles at the excitation of illumination.

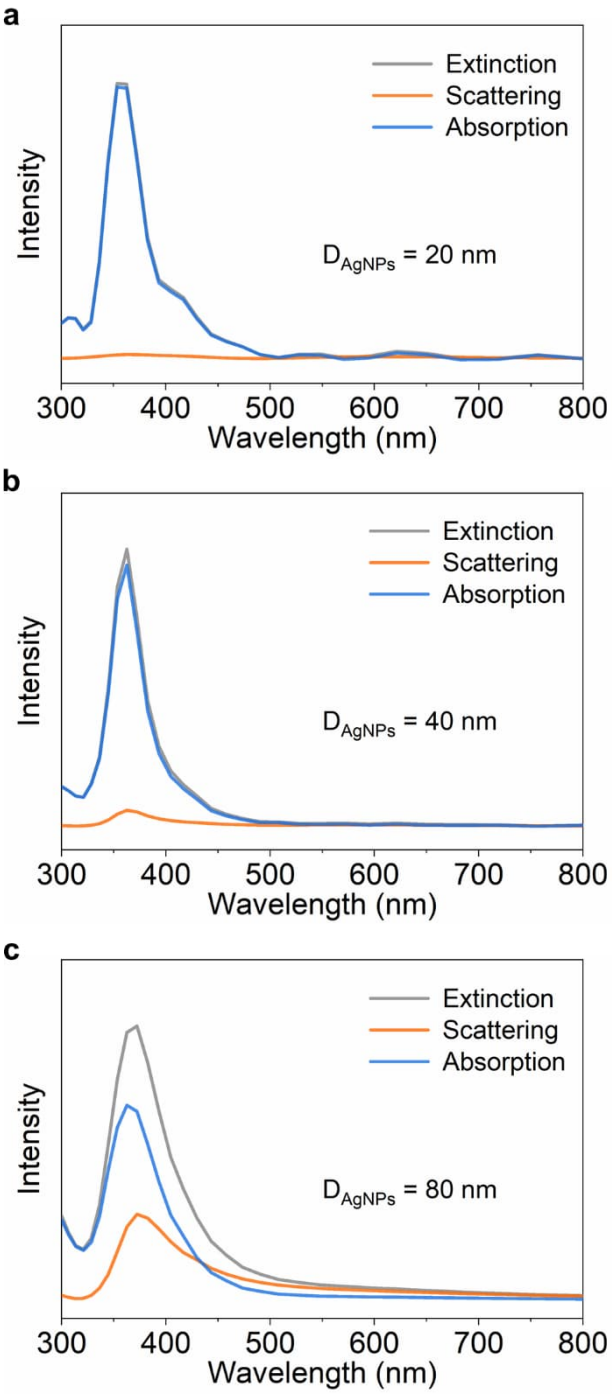

Figure S12. Extinction, scattering, and absorption spectra of Ag nanoparticles (diameters: 20, 40, and 80 nm) calculated using the finite difference time domain method.

The simulation results revealed that the scattering effect played an important role for Ag nanoparticles in 80 nm. The Ag nanoparticles in 80 nm allowed for the increased absorption of scattered light for TiO_2, leading to effective light utilization and more charge carrier generation.

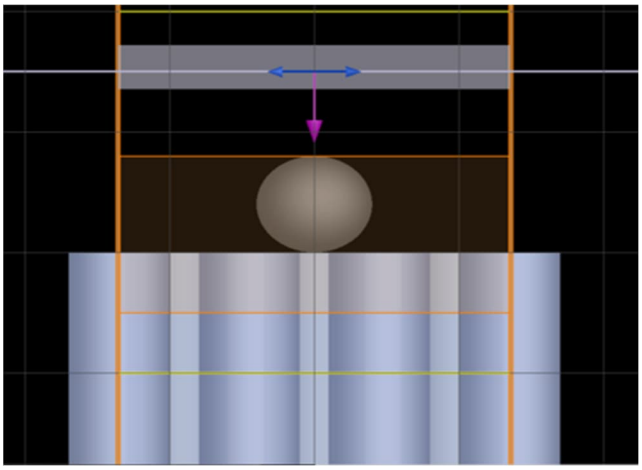

Figure S13. Schematic of the geometry model used in the finite difference time domain simulation. The purple arrow represents the direction of the incident light and blue arrow for the polarization orientations of electric field.

Figure S14. Power density of the light source used in this study.

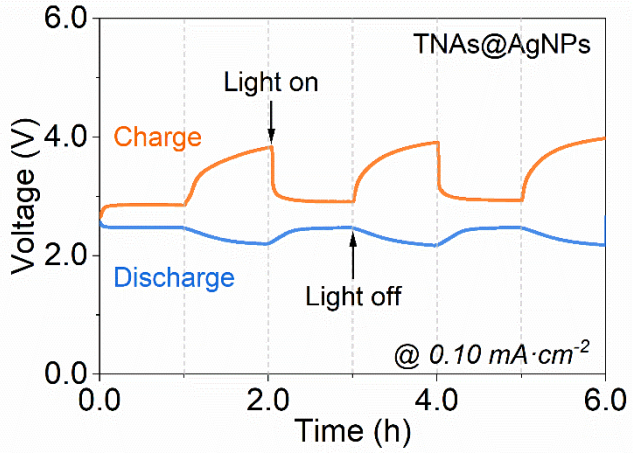

Figure S15. Discharge and charge profiles of Li-CO_2 batteries based on TNAs@AgNPs cathode responding to the intermittent light on and off.

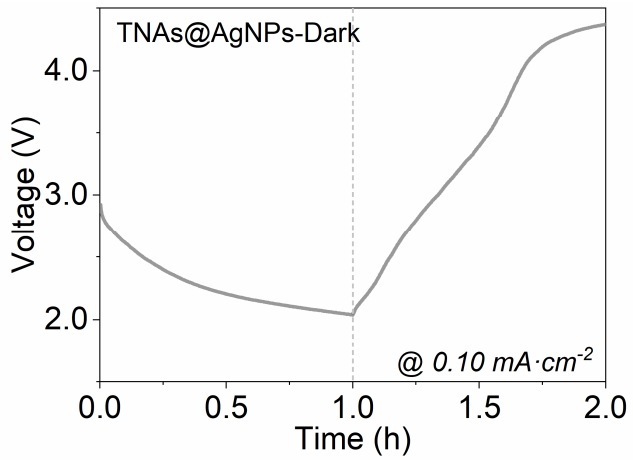

Figure S16. Discharge and charge profiles of Li-CO_2 batteries based on TNAs@AgNPs cathode in dark.

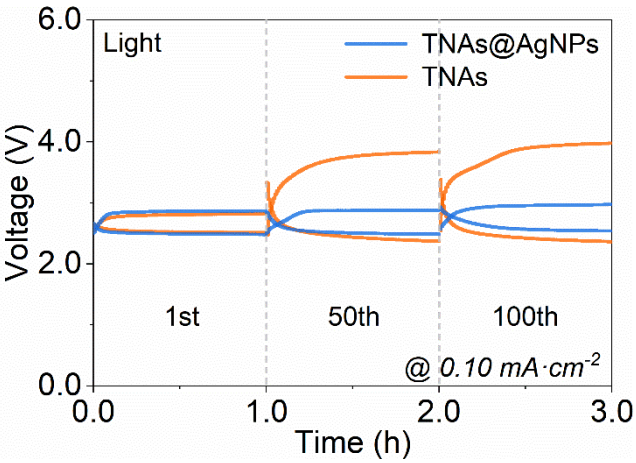

Figure S17. Cycling performance of Li-CO_2 batteries based on TNAs and TNAs@AgNPs cathodes in light.

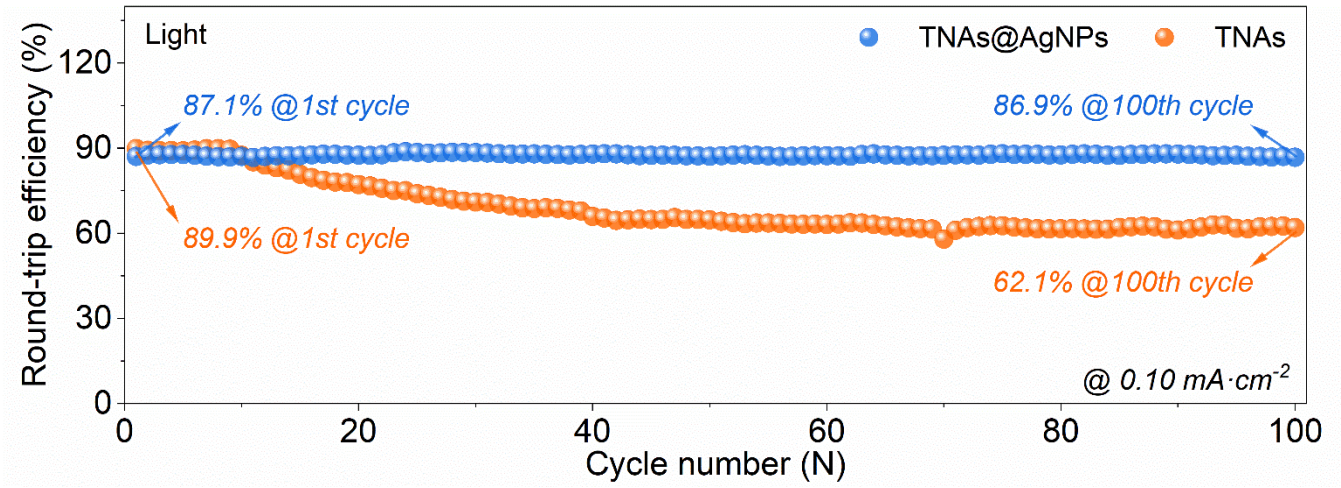

Figure S18. Round-trip efficiencies of Li-CO_2 batteries based on TNAs and TNAs@AgNPs cathodes in light. Representative round-trip efficiencies at the 1st and 100th cycles are marked in the inset for clarity.

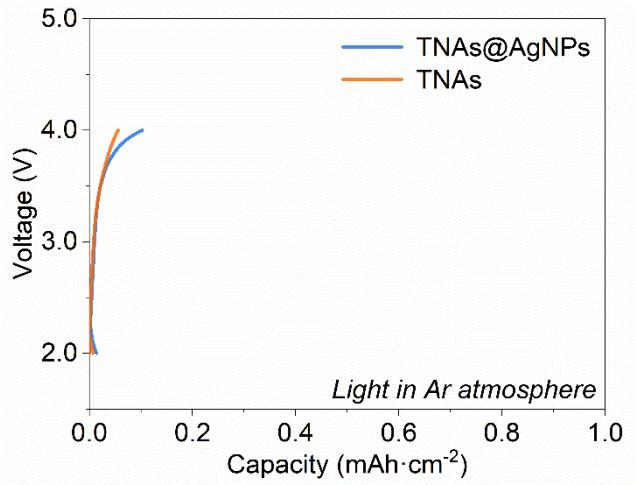

Figure S19. Discharge/charge profiles of Li-CO_2 batteries based on TNAs and TNAs@AgNPs cathodes under illumination in Ar atmosphere.

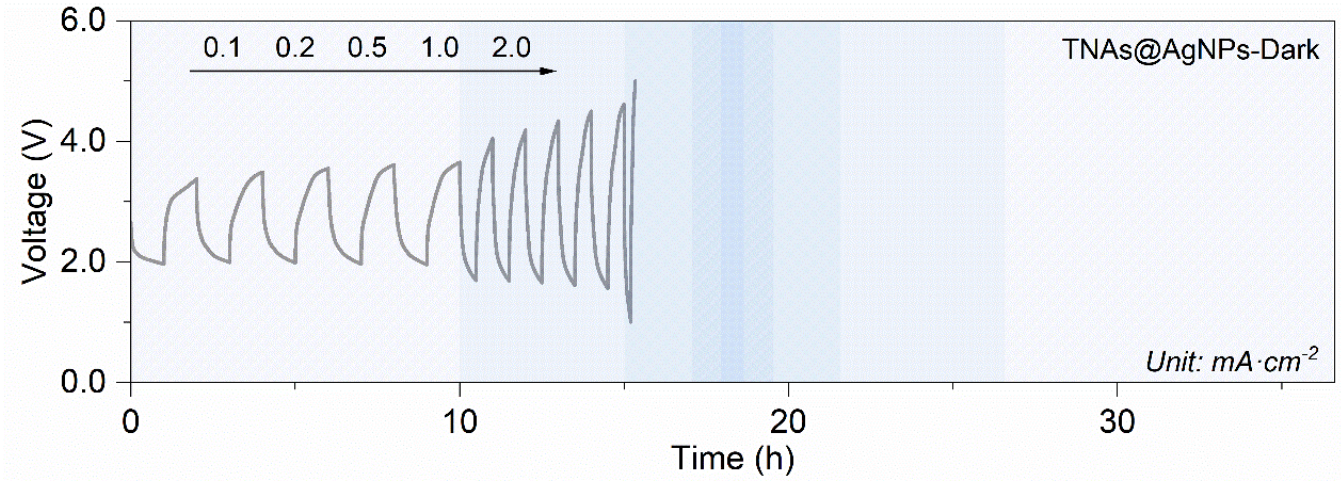

Figure S20. Rate performance of Li-CO_2 batteries based on TNAs@AgNPs cathode in dark.

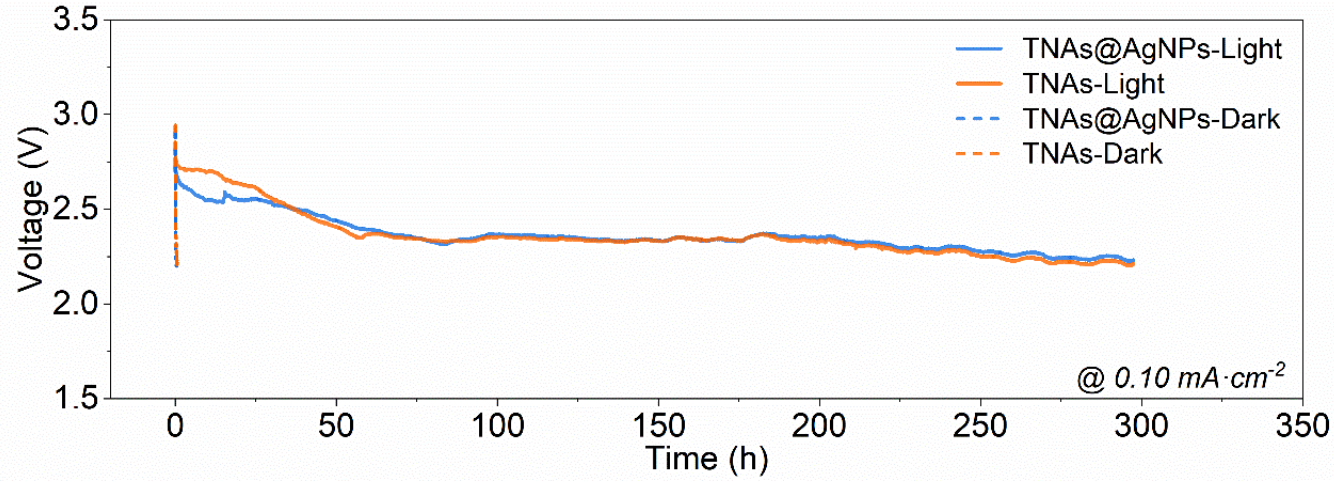

Figure S21. Deep discharge curves of Li-CO_2 batteries based on TNAs and TNAs@AgNPs cathodes in dark and light with a cut-off voltage of 2.2 V.

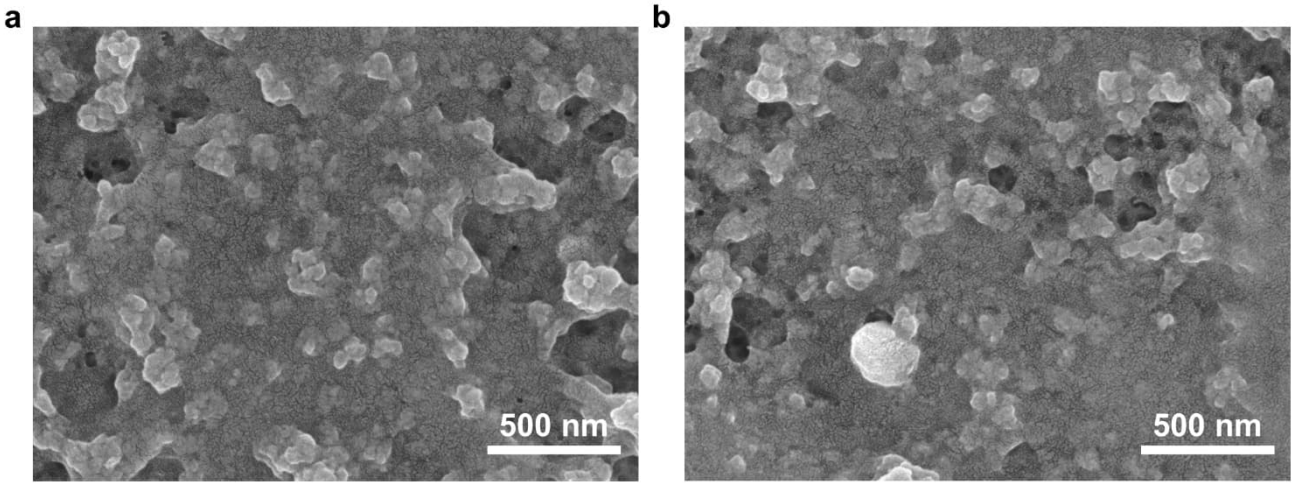

Figure S22. Scanning electron microscopy images of the discharged (**a**) TNAs and (**b**) TNAs@AgNPs cathodes without illumination.

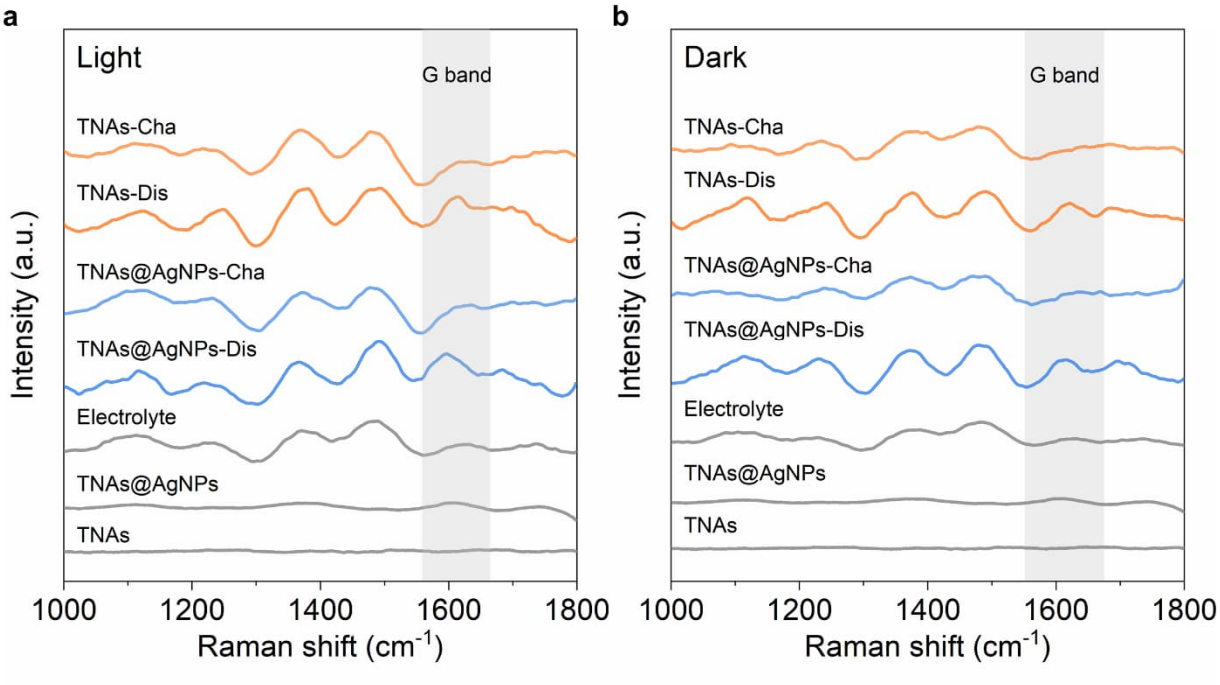

Figure S23. Raman spectra of TNAs@AgNPs and TNAs after discharging/charging (**a**) in light and (**b**) dark. Dis and Cha represent the cathodes disassembled from the discharged/recharged batteries, respectively.

For TNAs and TNAs@AgNPs cathodes in light, the formation/decomposition of carbon were confirmed based on the appearances/disappearances of D and G bands (around 1360 cm^{-1} and 1620 cm^{-1}, gray region). In comparison, high overpotentials triggered parasitic reactions associated with electrolyte in dark, resulting in the formation of indistinct characteristic peaks.

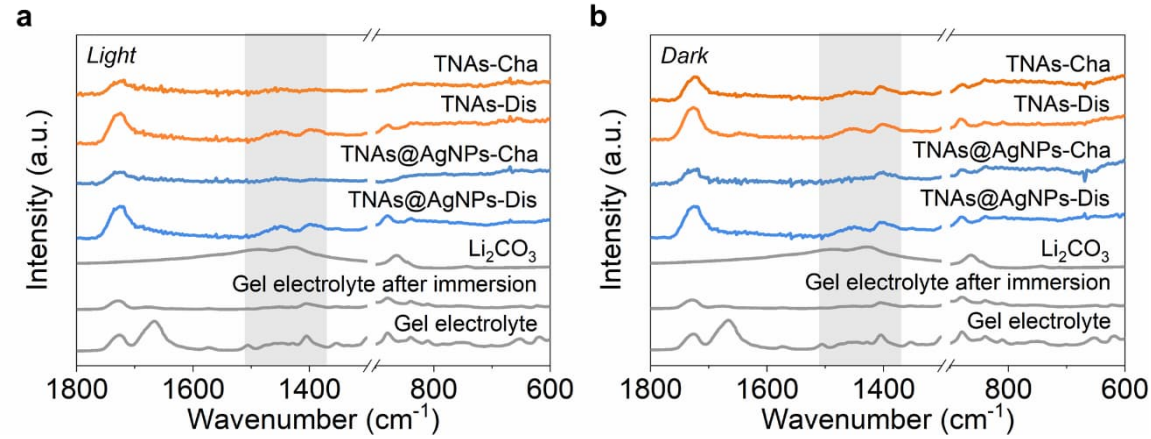

Figure S24. Infrared spectra of TNAs@AgNPs and TNAs cathodes after discharging/charging (**a**) in light and (**b**) dark.

The formation of Li_2CO_3 was confirmed based on the newly emerged peaks at 865, 1395, and 1450 cm^{-1} at the discharged TNAs and TNAs@AgNPs cathodes with/without illumination. The disappeared Li_2CO_3 signals after charging in light proved the enhanced CO_2 evolution kinetics under illumination, in contrast to the remained product signals in dark.

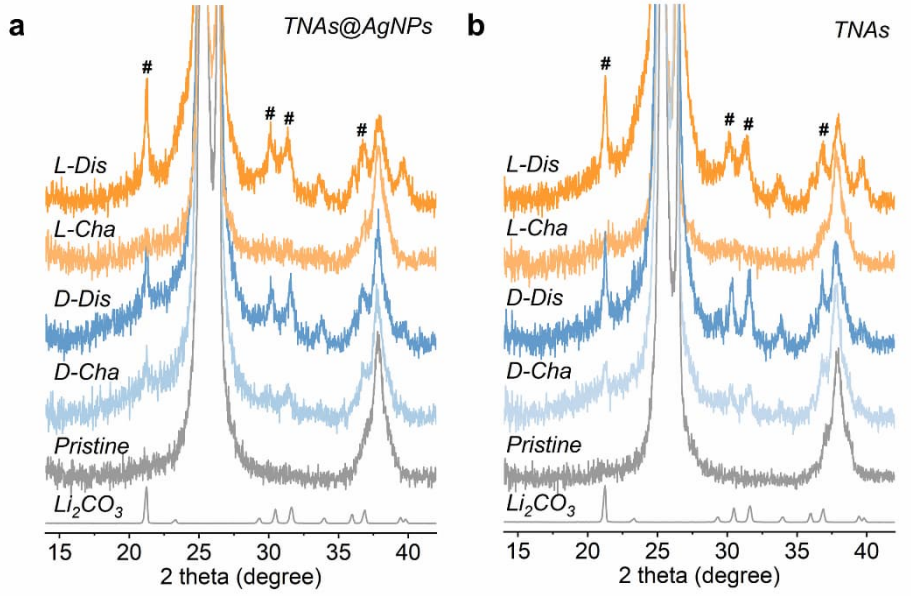

Figure S25. X-ray diffraction patterns of (**a**) TNAs@AgNPs and (**b**) TNAs after discharging/charging in light and dark. *L* and *D* represent the batteries working in light and dark. *Dis* and *Cha* represent the cathodes dissembled from the discharged/recharged batteries, respectively.

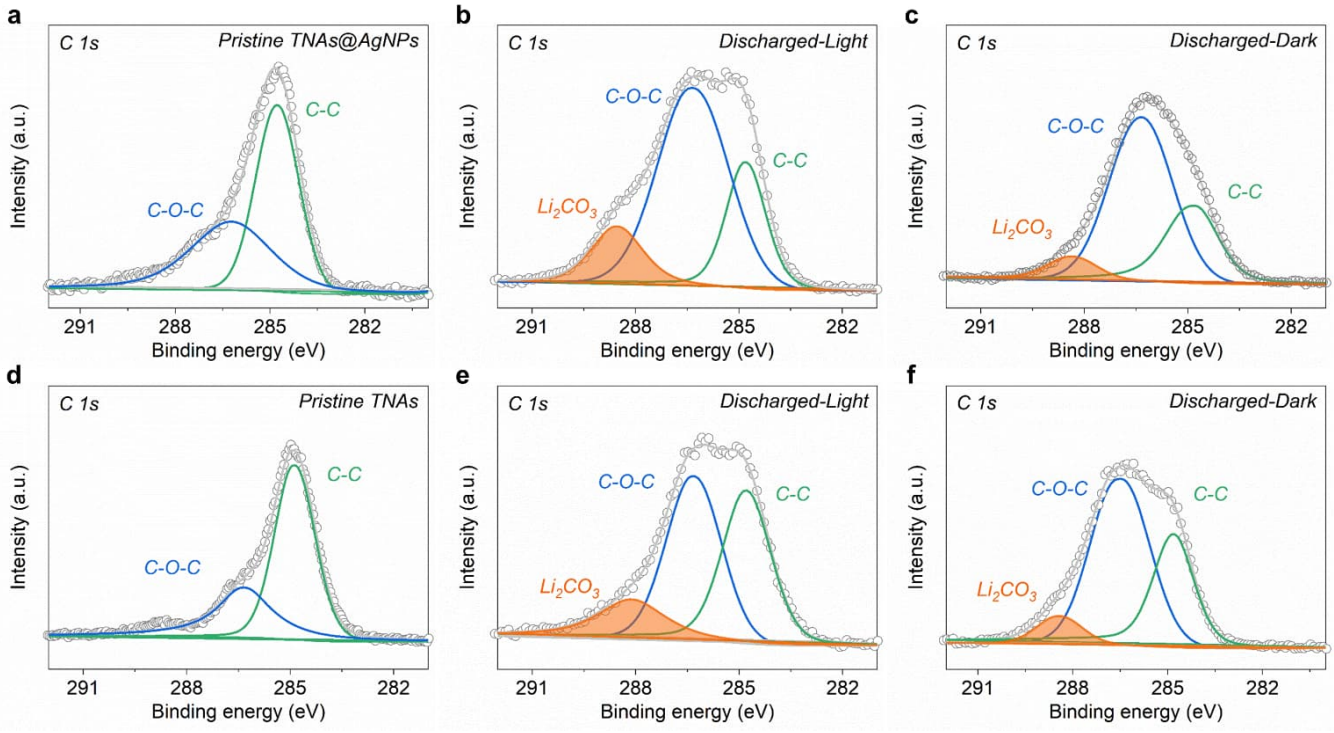

Figure S26. C 1s photoelectron spectra of pristine and discharged (**a**-**c**) TNAs@AgNPs and (**d**-**f**) TNAs cathodes in light and dark.

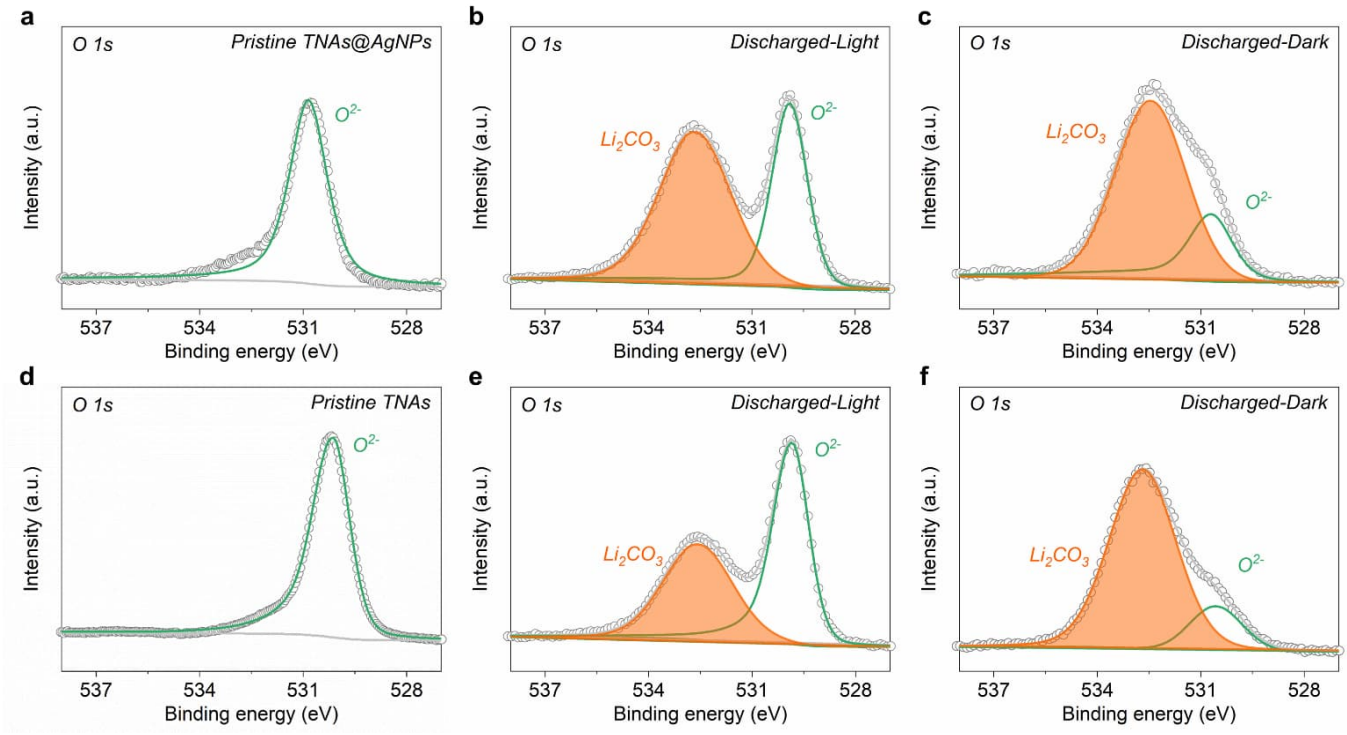

Figure S27. O 1s photoelectron spectra of pristine and discharged (**a**-**c**) TNAs@AgNPs and (**d**-**f**) TNAs cathodes in light and dark.

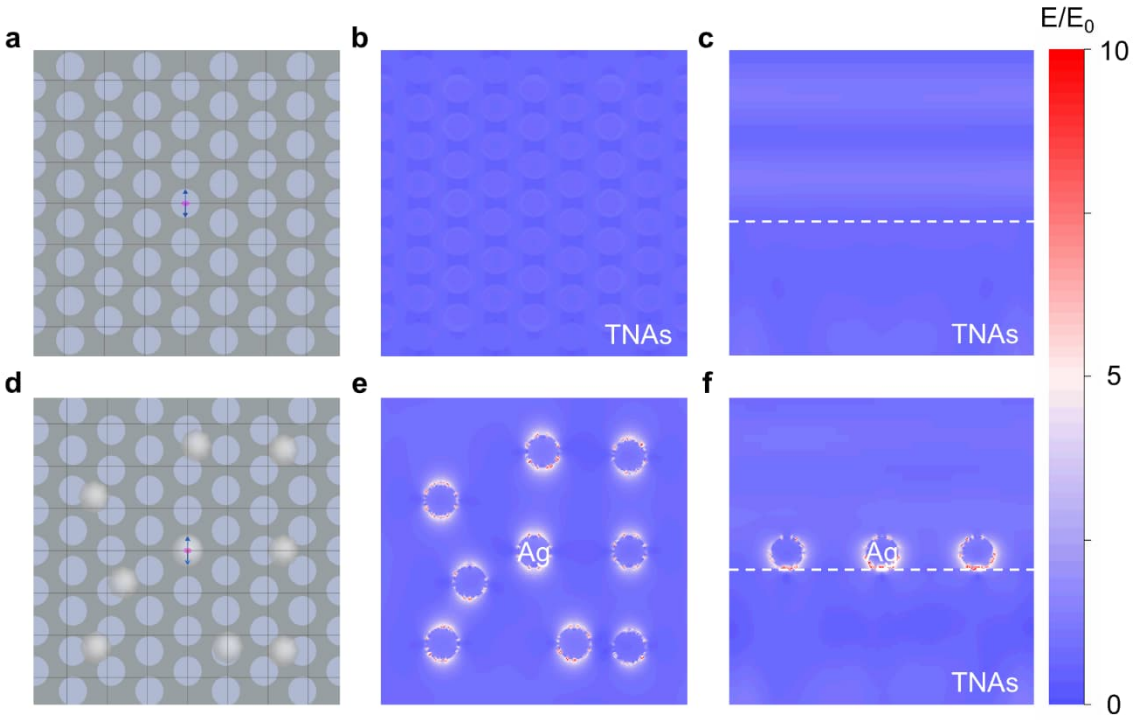

Figure S28. Finite difference time domain method simulations of (**a-c**) TNAs and (**d-f**) TNAs@AgNPs cathodes. E_0 and E represent the intensities of the incident and localized electric field, respectively.

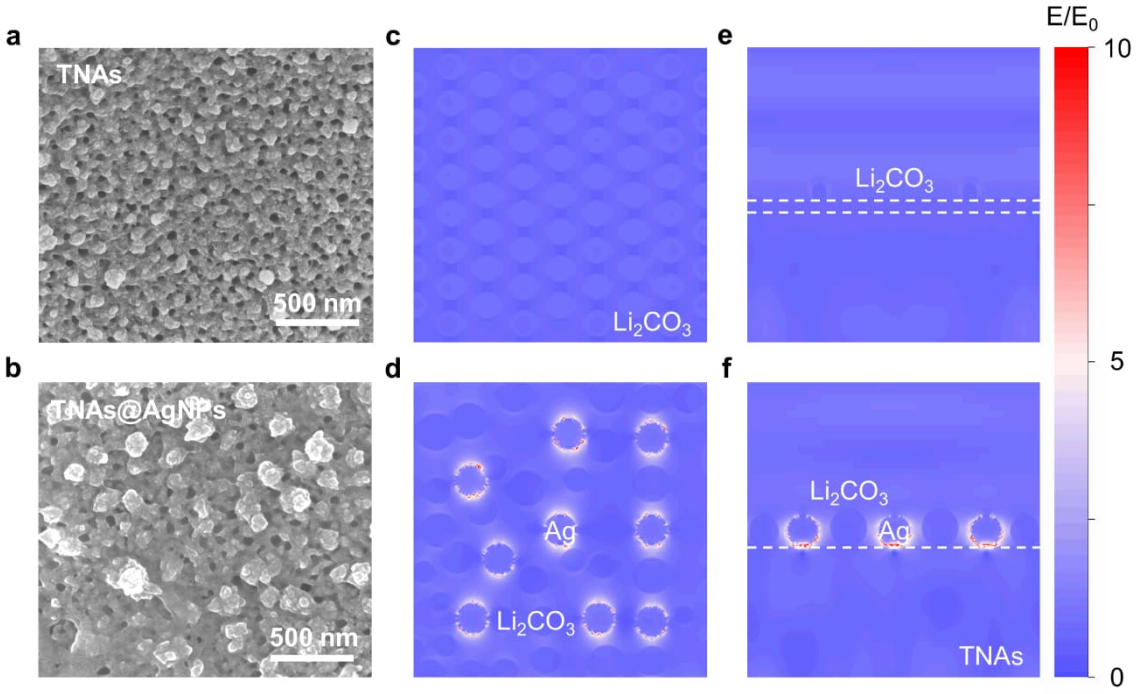

Figure S29. Scanning electron microscopy images of (**a**) TNAs and (**b**) TNAs@AgNPs cathodes after discharging to 0.025 mAh·cm^{-2} at 0.10 mA·cm^{-2}. Finite difference time domain method simulations of discharged (**c**, **e**) TNAs and (**d**, **f**) TNAs@AgNPs. E_0 and E represent the intensities of the incident and localized electric field, respectively.

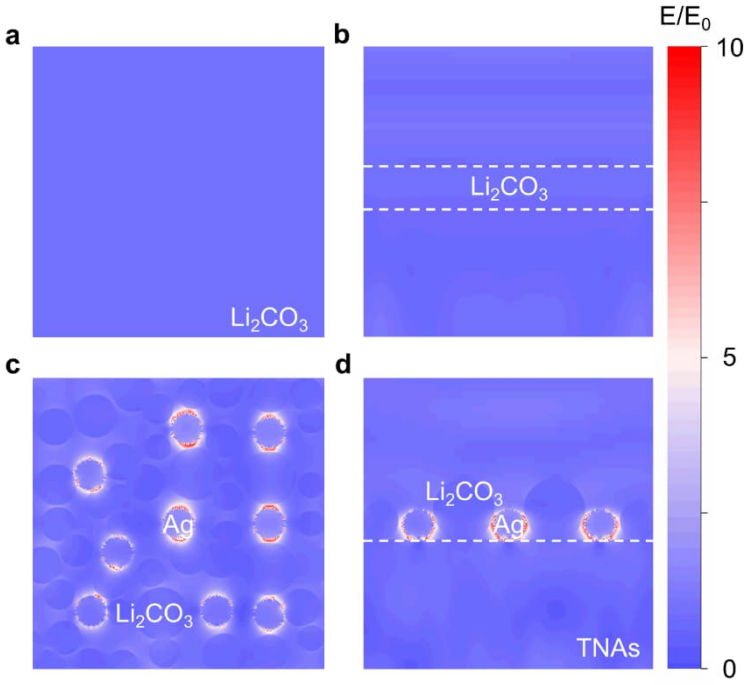

Figure S30. Finite difference time domain method simulations of the discharged (**a**, **b**) TNAs and (**c**, **d**) TNAs@AgNPs cathodes. E_0 and E represent the intensities of the incident and localized electric field, respectively.

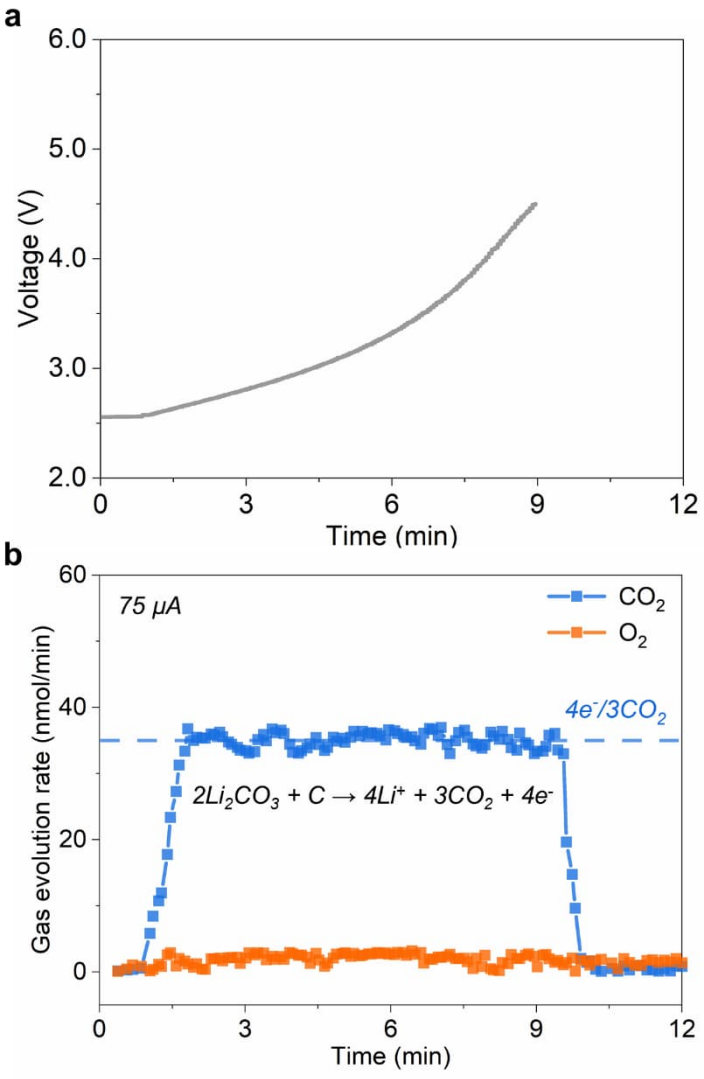

Figure S31. Differential electrochemical mass spectrometry result of gas evolution rates for CO_2 and O_2 during charging. The electron number (*versus* CO_2 gas molecule) marked with the dashed line corresponds to the related reaction pathway.

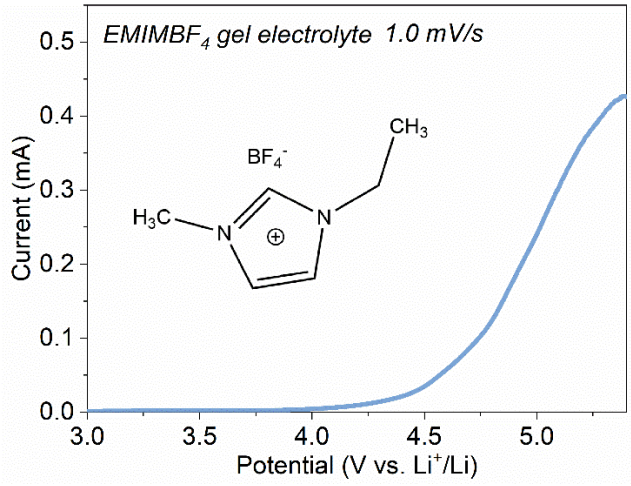

Figure S32. Linear sweep voltammetry curve of $EMIMBF_4$ gel electrolyte.

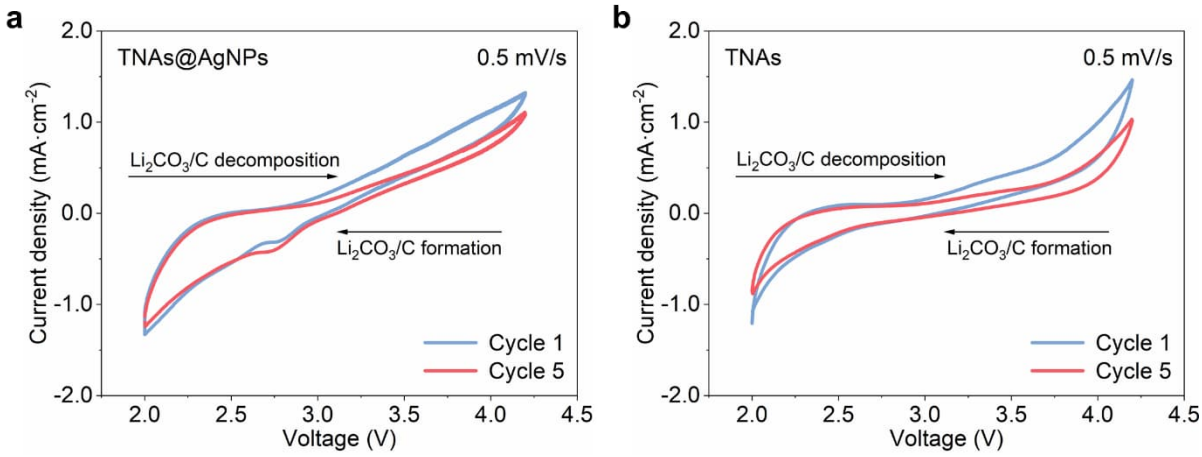

Figure S33. Cyclic voltammetry curves of the Li-CO_2 batteries based on (**a**) TNAs@AgNPs and (**b**) TNAs cathodes in light.

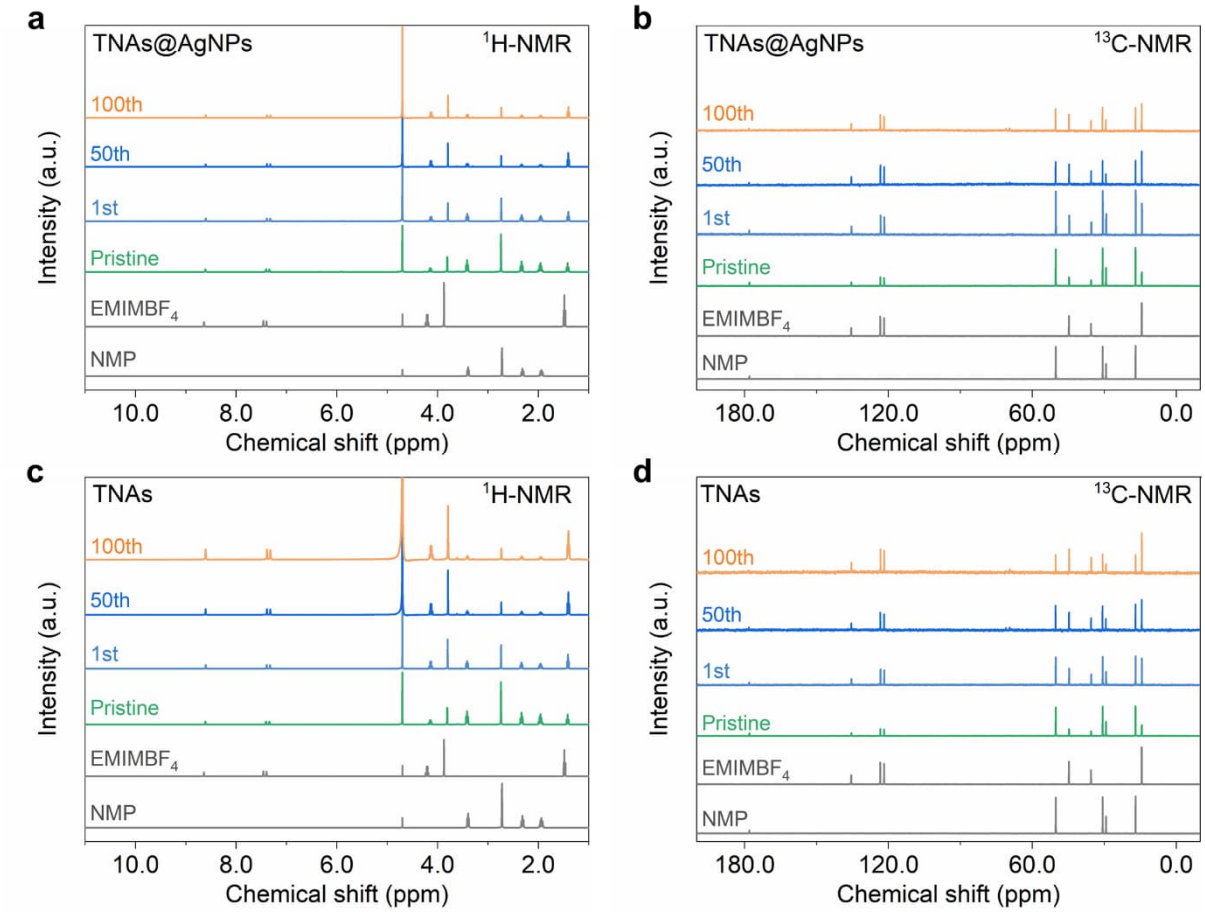

Figure S34. ^{1}H and ^{13}C NMR spectra of the deuterium water-extracted electrolytes from the cycled batteries based on (**a**, **b**) TNAs@AgNPs and (**c**, **d**) TNAs in light.

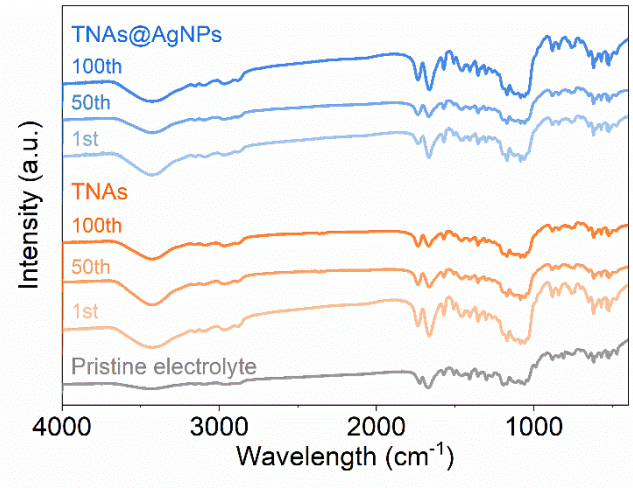

Figure S35. Infrared spectra of the pristine and cycled electrolytes from the cycled batteries with TNAs@AgNPs and TNAs in light.

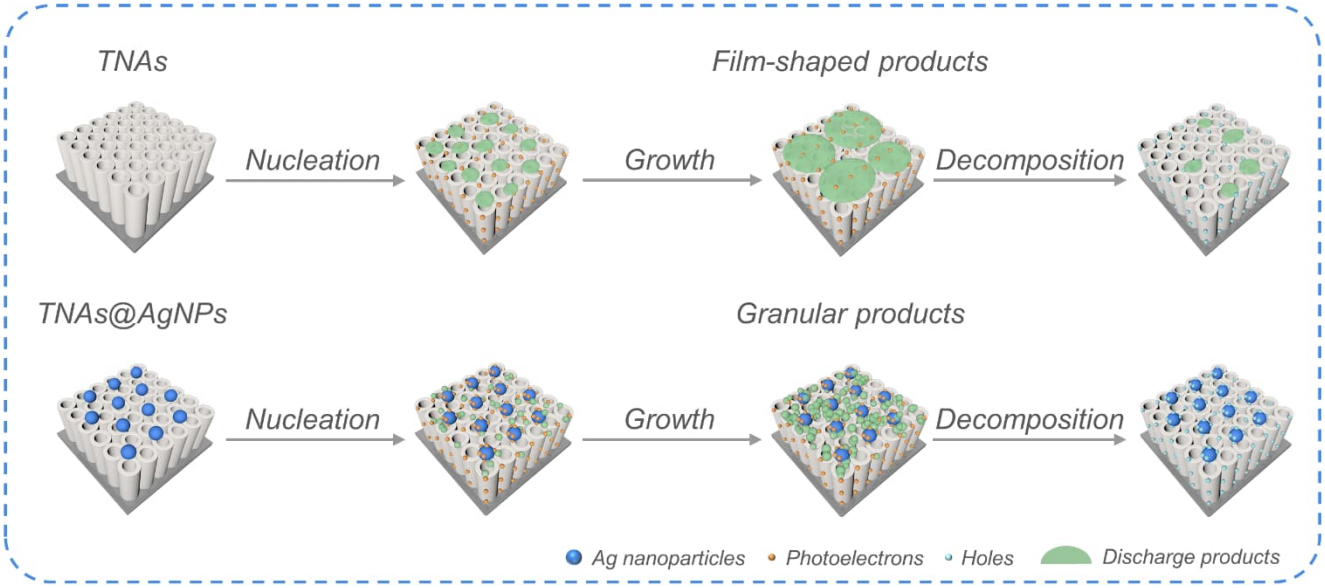

Figure S36. Schematics of the discharge/charge processes at the TNAs and TNAs@AgNPs cathodes.

Combining the product morphology evolution results and density functional theory calculations, the discharge products were speculated to follow the surface- and solution-mediated growth pathways at the TNAs and TNAs@AgNPs in light, respectively. For TNAs, the discharge products tended to nucleate uniformly at the cathode surface and grow to be film-shaped owing to the photoelectrons' uniform distribution. The film-shaped products fully covering the TNAs cathode decreased the reactive sites and hampered the decomposition of products upon charging, leading to the undecomposed film-shaped residuals at the TNAs cathode after charging. In comparison, for the TNAs@AgNPs, the discharge products tended to first nucleate and gather into particles in the electrolyte due to the locally intensified electric field around Ag nanoparticles, and deposit on the cathode surface. The TNAs@AgNPs cathode covered by the particle products remained reactive surface for the following full decomposition of products during charging.

Table S1. Properties comparison with some representative Li-CO_2 batteries.

Cathodes	Light sources	Current density ($mA \cdot cm^{-2}$)	Cut-off capacity ($mAh \cdot cm^{-2}$)	Cycling stability (Round-trip efficiency retention)	Rate performance ($mA \cdot cm^{-2}$)	Capacity ($mAh \cdot cm^{-2}$)	*Ref.*
TNAs@AgNPs (Photoelectrocatalysis)	**400 W Ultraviolet lamp**	**0.10**	**0.10**	**86.9%, 100th**	**2.00**	**31.11**	**This work**
TiO_2/CC (Photoelectrocatalysis)	300 W Xenon arc lamp	0.01	0.01	~95%, 30th	1.20	2.00	[4]
Cu_2O/CNT (Photoelectrocatalysis)	500 W Xenon lamp	0.04	0.40	~86%, 50th	0.05	/	[5]
In_2S_3@CNT/SS (Photoelectrocatalysis)	/	0.01	0.01	~80%, 24th	0.50	2.50	[6]
SiC/RGO (Photoelectrocatalysis)	500 W Xenon lamp	0.01	0.01	~70%, 80th	0.20	3.25	[7]
Fe-ISA/N, S-HG (Electrocatalysis)	/	0.21	0.21	~62%,100th	0.42	4.87	[8]
Graphene@COF (Electrocatalysis)	/	0.08	0.16	~52%, 56th	0.16	2.73	[9]
Ir-CNFs (Electrocatalysis)	/	0.04	0.20	~58%, 50th	0.04	4.31	[10]
Ni-NG (Electrocatalysis)	/	0.04	0.40	~59%, 100th	0.07	6.17	[11]
Graphene (Electrocatalysis)	/	0.02	0.36	~64%, 20th	0.04	5.30	[12]

Note S1. Structural information of the intermediates in the DFT calculations (a = 10.8858 Å, b = 11.3280 Å, c = 23.8448 Å, α = 90.0000° β = 90.0000° γ = 110.2962°).

TiO_2			TiO_2 + Ag		
0.23267559	0.24448272	0.03024966	0.23636329	0.24598677	0.03016468
0.37076935	0.29033047	0.18569356	0.38100312	0.29329178	0.18564251
0.00362787	0.00148205	0.05935711	0.00644219	0.00154712	0.05699071
0.14100968	0.04631935	0.21474613	0.14984322	0.0506179	0.21188879
0.73268343	0.24446093	0.03026055	0.73441174	0.24522662	0.02808324
0.8707595	0.29029139	0.18572006	0.88095732	0.29293229	0.1807933
0.50364896	0.00149966	0.0593649	0.50779799	0.00186601	0.05926342
0.64097247	0.04630468	0.21475129	0.65270485	0.05300511	0.2130272
0.23274464	0.57768363	0.03028029	0.23845267	0.57990636	0.03125178
0.37041693	0.62343312	0.18590165	0.38356368	0.6263802	0.18820124
0.003305	0.33464796	0.05950979	0.00588421	0.33556977	0.05542648
0.14124458	0.37968946	0.21519528	0.15113759	0.38325116	0.21158055
0.73274249	0.57768308	0.03027127	0.73344608	0.57847463	0.03024038
0.87040735	0.62341566	0.18589776	0.87734722	0.62725474	0.18140923
0.50332129	0.33466429	0.05949564	0.50667798	0.33546737	0.05901139
0.64125495	0.37971105	0.21519786	0.65433505	0.38120486	0.21250486
0.23303985	0.9111393	0.03007218	0.2373466	0.91228875	0.03061927
0.37041937	0.95693633	0.18564977	0.38025125	0.95996686	0.18624371
0.00346008	0.66832926	0.05925162	0.00721166	0.66899724	0.05636167
0.14113868	0.71336273	0.21499336	0.14994808	0.71579615	0.21335448
0.73301692	0.91112165	0.03007338	0.73465763	0.90903359	0.03014789
0.87045642	0.9569223	0.18565874	0.87944541	0.96212023	0.18415382
0.50345979	0.66832546	0.05924874	0.50595538	0.66852478	0.06541718
0.64111322	0.71334153	0.21499882	0.65569309	0.72359042	0.22266507
0.04646217	0.18227762	0.06119376	0.04727386	0.1824919	0.05824509
0.19258352	0.23023803	0.22652126	0.2022528	0.23448762	0.22546557
0.32620511	0.27566778	0.09796014	0.33036522	0.27635081	0.09805352
0.47813085	0.32604105	0.25063752	0.49113029	0.33443514	0.25021002
0.18138405	0.06077258	0.01848616	0.18620526	0.06206046	0.01830187
0.32745581	0.10920936	0.18382025	0.33815711	0.11287097	0.18421173
0.39582365	0.29836224	-0.0052981	0.39860633	0.3015635	-0.0056871
0.04738019	0.01541469	0.14709955	0.05584771	0.01984805	0.14460026
0.54647576	0.18228067	0.06120027	0.54899639	0.18279752	0.05870061
0.69256371	0.23021199	0.22652743	0.71009645	0.23552125	0.22743894
0.82621881	0.27566535	0.09797267	0.83025371	0.27965637	0.09527741
0.97813334	0.32603452	0.25065278	0.98683663	0.32661364	0.24916407
0.68139136	0.06077109	0.01849164	0.68590207	0.06107488	0.01883376
0.82745398	0.10918513	0.18385058	0.8357059	0.1137794	0.17711068
0.89584666	0.29837886	-0.0052895	0.89655684	0.29871719	-0.0085119

0.5473737	0.01540652	0.14710393	0.55433682	0.01893344	0.14615282
0.04616519	0.51560482	0.06101073	0.04684319	0.5156968	0.05874027
0.19232574	0.5636977	0.22655305	0.19694863	0.56407248	0.22613405
0.326291	0.60908311	0.0979332	0.32551222	0.61056911	0.10055718
0.47815706	0.65930862	0.25066618	0.48134601	0.64877513	0.25632494
0.18094773	0.39387767	0.01852108	0.18524272	0.39553835	0.01787598
0.32715867	0.44228224	0.18398832	0.33658937	0.44457174	0.18342235
0.39565184	0.63205943	-0.0054621	0.40140814	0.6318455	-0.0019497
0.04769724	0.34919135	0.14738446	0.05699658	0.35111902	0.14413021
0.5461588	0.51559796	0.06100876	0.55065663	0.51566713	0.06414661
0.69233782	0.56370968	0.22655106	0.70328907	0.56089485	0.22058925
0.82630335	0.60909187	0.09793007	0.8321358	0.61349678	0.097244
0.97816495	0.65933315	0.25066167	0.98487316	0.66178018	0.25039479
0.68095195	0.39386705	0.0185221	0.68335166	0.3957512	0.0173442
0.82717695	0.44227397	0.18399587	0.84114027	0.44592536	0.18052891
0.89566201	0.63205383	-0.0054665	0.89559362	0.63274955	-0.0066572
0.5477185	0.3492149	0.14737612	0.55583439	0.34382881	0.14597266
0.0465291	0.84906214	0.06093307	0.04967491	0.84937578	0.05944748
0.19284448	0.89739589	0.22662033	0.19858026	0.89992003	0.22503171
0.32618051	0.94210743	0.09784689	0.33059279	0.94118755	0.09854398
0.47809225	0.99229113	0.250463	0.48991393	0.00071913	0.25006277
0.18129526	0.72728828	0.01852121	0.18575952	0.72849898	0.0177446
0.32738543	0.77572771	0.18397508	0.33826012	0.77895351	0.18859254
0.39600957	0.9657314	-0.0055014	0.39928412	0.96528792	-0.0053938
0.04742888	0.68269813	0.14730618	0.05732757	0.68575885	0.14577205
0.54652616	0.84906738	0.06093424	0.54997725	0.8498942	0.06159052
0.69283985	0.89739174	0.22662653	0.71044754	0.91457526	0.22968741
0.82617281	0.94209894	0.09784174	0.83118577	0.93862983	0.09708182
0.97812876	0.99229447	0.25045743	0.98929121	0.00288138	0.24883279
0.68128458	0.72727795	0.01851863	0.68141298	0.72573948	0.01993449
0.82739221	0.77572442	0.18396776	0.84046019	0.78209863	0.18663076
0.89599059	0.96571669	-0.0055084	0.89654042	0.96317773	-0.0067853
0.54741973	0.68270347	0.14731386	0.54942362	0.6869025	0.14935573
			0.68360738	0.40552906	0.38496354
			0.87423615	0.35352863	0.32638873
			0.56005851	0.53841617	0.32477049
			0.83618382	0.58323057	0.31917895
TiO_2 + $LiCO_2$			**TiO_2 + Ag + $LiCO_2$**		
0.22438043	0.24326774	0.03457019	0.22580726	0.24261552	0.03143103
0.36756683	0.2908087	0.18882534	0.37039819	0.2912221	0.18499679
0.99653851	-0.0006746	0.06254303	0.99839974	0.00024124	0.06069854
0.14367906	0.04720907	0.21710135	0.14396527	0.04561564	0.21467816

0.72809901	0.24507008	0.03340204	0.72980252	0.24407261	0.0313597
0.8746743	0.29380946	0.19058073	0.87357291	0.28930415	0.18733337
0.49621573	0.00085882	0.05841708	0.49757224	0.00052252	0.05899023
0.64418776	0.0510983	0.21281391	0.64197823	0.04496113	0.2137202
0.22247846	0.5737991	0.0344247	0.22446761	0.57455282	0.03060975
0.36569731	0.62461071	0.18726526	0.36379809	0.62060299	0.18284565
0.99528894	0.33192886	0.06784777	-0.0018829	0.33297753	0.06643734
0.14306142	0.38380225	0.22628962	0.14269505	0.37810681	0.22900069
0.72611841	0.5773217	0.03347539	0.72574452	0.57535593	0.03179067
0.86911969	0.62411193	0.18856161	0.86980373	0.62481687	0.18535519
0.49615267	0.33363967	0.06141231	0.49697579	0.33207068	0.05985765
0.6389104	0.38016769	0.21587574	0.64586919	0.38065021	0.21523888
0.22418363	0.90880955	0.0323454	0.22686786	0.9092103	0.03134898
0.37056868	0.9577532	0.18506838	0.37318212	0.95801408	0.1862145
0.99610421	0.66617035	0.06246918	0.99765738	0.66634476	0.05931007
0.14050526	0.71750909	0.21664667	0.14402349	0.71786189	0.21504456
0.72628943	0.91026938	0.03374992	0.72802925	0.91017457	0.03172661
0.8725913	0.95838981	0.18949492	0.87247199	0.95605357	0.1873796
0.49514099	0.66628261	0.06006583	0.49685455	0.66692989	0.05730811
0.64136655	0.71451867	0.21388705	0.63852327	0.71399799	0.21219134
0.03922321	0.17941716	0.06603366	0.04121649	0.1803044	0.06385537
0.19674054	0.22497744	0.23104489	0.1941786	0.22373614	0.2259474
0.32079011	0.2780164	0.1018272	0.32106561	0.27211989	0.0989673
0.47827369	0.32565286	0.2532014	0.47814665	0.34438939	0.25364868
0.17423207	0.0594612	0.02186988	0.17495528	0.05872368	0.01929777
0.33017712	0.1093704	0.18459318	0.331938	0.10979587	0.18441159
0.38576341	0.2974912	0.997633	0.38763079	0.29685526	0.9951968
0.04604506	0.0134939	0.15002155	0.0465627	0.01057063	0.14783262
0.53678984	0.18058757	0.06109361	0.53947734	0.1803144	0.06058212
0.6861183	0.22842492	0.2275763	0.68463474	0.22600662	0.22351533
0.81526054	0.27403265	0.10259161	0.81754762	0.27326196	0.10058306
0.96822059	0.32465639	0.25719352	0.95779796	0.31958179	0.25868289
0.67533661	0.05966581	0.02081436	0.67710478	0.05990473	0.0196588
0.82887821	0.10951831	0.18695002	0.82843527	0.10665394	0.18578501
0.89103284	0.29678882	0.00015909	0.8931562	0.29849807	0.99849302
0.54651508	0.01968543	0.14682817	0.54708421	0.01217302	0.14676769
0.03776404	0.51388131	0.06502663	0.04141241	0.51530926	0.0637427
0.19946576	0.57911849	0.23313711	0.18940292	0.57011336	0.22515513
0.3201919	0.60380025	0.10142411	0.32175793	0.60909647	0.09764078
0.47988134	0.67855404	0.25323407	0.47511206	0.64730018	0.24981543
0.17244011	0.39154006	0.02410065	0.17452724	0.39195229	0.0216949
0.33082389	0.44699726	0.19223129	0.32760342	0.44262603	0.18588358

0.38405048	0.62943713	0.99703626	0.38711153	0.62892303	0.99379698
0.04109186	0.34989561	0.1516198	0.0407117	0.34730575	0.15101667
0.53863155	0.5147085	0.06260546	0.53900131	0.51370728	0.06112058
0.68750351	0.56533212	0.22809073	0.6922725	0.56698805	0.22576805
0.81958347	0.60775569	0.10140652	0.82206259	0.60646127	0.09934214
0.97744329	0.66564636	0.2529706	0.9779497	0.66722983	0.25343347
0.67540495	0.39432692	0.0217945	0.67538307	0.39282896	0.01960235
0.82655658	0.4448896	0.1892603	0.83082967	0.44506898	0.18664942
0.88850507	0.63159348	0.99768793	0.8883586	0.62846743	0.99539732
0.54467861	0.35023095	0.14887526	0.5439251	0.34675628	0.14728987
0.03963997	0.84718137	0.06398587	0.04024624	0.84674223	0.06118536
0.20004479	0.90071542	0.23133249	0.19836652	0.89909703	0.22952623
0.32128182	0.94299465	0.09925947	0.32228273	0.94136902	0.09870927
0.48100022	0.98050847	0.25167156	0.48024097	0.99175203	0.25093454
0.17376818	0.72487266	0.02212451	0.17494262	0.72529734	0.01877397
0.32545744	0.77830317	0.18149617	0.32692983	0.77660783	0.18331489
0.38533144	0.96133573	0.99503052	0.38865678	0.96408051	0.99472828
0.04404559	0.68316795	0.14942817	0.04503075	0.68711141	0.1485457
0.53785379	0.84742844	0.06287078	0.53977919	0.8475227	0.05960572
0.69052427	0.89832458	0.23115248	0.69169552	0.89456223	0.22798612
0.82015063	0.94104227	0.10157961	0.82182503	0.94109231	0.09948301
0.97994363	0.99123432	0.25367362	0.98034247	0.98866279	0.25161818
0.6739816	0.72654164	0.02101463	0.67695961	0.72585022	0.01920628
0.82554823	0.77722908	0.18593902	0.82501227	0.77500531	0.18289756
0.88859534	0.96322193	0.99789282	0.89020787	0.96549784	0.9958451
0.54375148	0.68095485	0.14832001	0.54339286	0.68608452	0.14556386
0.49462391	0.82698775	0.37339247	0.39773171	0.48272288	0.37570325
0.489749	0.79271846	0.47066936	0.23187547	0.40850581	0.3125961
0.49716477	0.83601022	0.28571512	0.28206815	0.44866904	0.35997776
0.4921711	0.80955503	0.42219842	0.42390653	0.48280082	0.2847216
			0.8821778	0.62172413	0.33501785
			0.87697296	0.37777562	0.33242774
			0.75405117	0.53504061	0.42931494
			0.63773349	0.39887572	0.33513422
$TiO_2 + LiC_2O_4$			**$TiO_2 + Li_2C_2O_4$**		
0.22569863	0.24228136	0.03181682	0.22588089	0.24256478	0.0319135
0.36464534	0.28976849	0.18473902	0.36470415	0.28984679	0.18469736
0.99833612	0.99960593	0.06151312	-0.0016409	-0.0002039	0.06100972
0.13999476	0.04436536	0.21559237	0.13977362	0.04452396	0.21519781
0.73115509	0.24438333	0.03286682	0.73205722	0.24465482	0.03278614
0.87201522	0.290871	0.18843132	0.87309249	0.29146931	0.18880312
0.49854116	0.00093157	0.06011673	0.49872953	0.00128665	0.05955107

0.64034516	0.04687194	0.21557899	0.64024826	0.04734633	0.21506232
0.2257605	0.57530523	0.0313816	0.22584399	0.57543916	0.03152843
0.3636923	0.61978188	0.18440119	0.36354892	0.61991369	0.18437646
0.00029581	0.33360314	0.06595858	0.00072656	0.3338652	0.06701452
0.13882902	0.37987091	0.22670353	0.14063516	0.38064987	0.22850205
0.72856722	0.57614291	0.03168162	0.7284352	0.57584364	0.03139394
0.86959612	0.62371991	0.18731862	0.86929351	0.62368186	0.18708202
0.49777105	0.33272394	0.0583979	0.49809188	0.33268873	0.05839161
0.63918025	0.37968124	0.21366638	0.63906398	0.37957774	0.21367554
0.22754412	0.90945994	0.03183173	0.22748875	0.90960135	0.03176846
0.3710641	0.95693893	0.18686576	0.37110212	0.95703623	0.18673162
0.99835465	0.66642655	0.06109191	-0.0018079	0.66626639	0.06073522
0.14018851	0.71600737	0.21602714	0.13996799	0.71632944	0.21573876
0.72860671	0.91070176	0.03203892	0.72844528	0.91051778	0.03181381
0.86870149	0.95552895	0.18771952	0.86835644	0.9554075	0.18722781
0.49790259	0.666845	0.0582489	0.49809947	0.66677403	0.0583461
0.63803842	0.71257084	0.21342623	0.63756513	0.71251496	0.21350115
0.04281822	0.18078537	0.0653631	0.04321856	0.18084263	0.06552571
0.18736764	0.22537187	0.22413498	0.1877915	0.22524953	0.22425935
0.32264039	0.27385789	0.09870503	0.32306951	0.27378332	0.09871415
0.47551428	0.34127366	0.25096608	0.47555754	0.34009638	0.25099029
0.17562397	0.0591326	0.02045698	0.17582491	0.05942632	0.02029163
0.32909247	0.11007775	0.18544494	0.32906813	0.10998289	0.18521727
0.3874126	0.29593243	0.99479222	0.38768825	0.2959611	-0.0051745
0.04426834	0.00968728	0.14827926	0.04414619	0.00930332	0.14793433
0.54165369	0.18145829	0.06170087	0.54214815	0.18160016	0.06154271
0.6861281	0.22982973	0.22617706	0.68650549	0.23000614	0.2269376
0.82139917	0.27380531	0.10170345	0.82110864	0.27412991	0.10195501
0.96991202	0.32490502	0.2557223	0.97002283	0.32413336	0.25641805
0.67784786	0.06072616	0.02063912	0.67807132	0.06079662	0.02018409
0.82783427	0.10878143	0.18795582	0.8275746	0.10894639	0.18747222
0.89512789	0.29840464	0.99941436	0.89626831	0.29874262	-0.0001074
0.54672668	0.01434346	0.14768357	0.54661226	0.01483453	0.14737285
0.04268116	0.51471939	0.06494325	0.04279439	0.51498717	0.06504897
0.18832251	0.56627933	0.22519353	0.18791423	0.5669633	0.22467531
0.32227568	0.60813728	0.09836832	0.32246401	0.60863372	0.09847565
0.47459217	0.64212569	0.25056834	0.47443653	0.64302004	0.25061431
0.17515019	0.39189067	0.02167866	0.17570211	0.39220812	0.02241077
0.31918204	0.43981725	0.18439128	0.31961758	0.43998382	0.18446504
0.38787771	0.62954306	0.99458068	0.38797881	0.62900785	-0.0053098
0.04577159	0.34896721	0.15343409	0.04575328	0.34944175	0.15392817
0.54047926	0.51384707	0.06069413	0.54078849	0.51380907	0.06078179

0.69003037	0.56373319	0.22727043	0.68998666	0.56373739	0.22732186
0.82148768	0.60600031	0.09949118	0.82146829	0.60570391	0.09925965
0.97685786	0.66231455	0.25152281	0.97676688	0.66269916	0.25152475
0.67704075	0.39238703	0.01930441	0.67727689	0.39233426	0.0190771
0.82598594	0.44278811	0.18600721	0.82615936	0.44290632	0.18637556
0.89133791	0.62893319	0.99609522	0.89122463	0.62884328	-0.0042178
0.5435904	0.34744534	0.14695605	0.54385933	0.34731854	0.14695834
0.04032509	0.8468956	0.06130992	0.04004893	0.8468596	0.06079927
0.19492478	0.89838	0.22851491	0.19517962	0.89884205	0.22870077
0.32216864	0.94105935	0.09936006	0.32252404	0.94114315	0.09913608
0.47810667	0.99193842	0.25154053	0.47839804	0.99216446	0.25147901
0.17579617	0.725398	0.02005074	0.17591515	0.72543408	0.01990882
0.32833572	0.77579332	0.18531291	0.32847289	0.7762112	0.18513307
0.38952719	0.96501093	0.99566869	0.38946321	0.96540255	-0.0046721
0.04523402	0.68649802	0.14829354	0.04495725	0.68694266	0.14810893
0.54013339	0.84749267	0.06012019	0.54016583	0.84755111	0.05995309
0.68809566	0.89427085	0.22707073	0.68820031	0.89462688	0.22705499
0.82111711	0.94184826	0.09996446	0.82110832	0.9417809	0.09965518
0.97726071	0.98893728	0.25173501	0.97701071	0.98911672	0.2514506
0.67786155	0.72654534	0.01974344	0.67782796	0.72633513	0.01968572
0.82312064	0.77414404	0.18399455	0.82274089	0.77409114	0.1839179
0.89138571	0.96683375	0.99650161	0.8912171	0.96687092	-0.0038581
0.54285898	0.68353559	0.1466111	0.54286475	0.68354517	0.14663688
0.11707059	0.35228023	0.42797138	0.11586171	0.36018624	0.43218092
0.11637114	0.53931812	0.38575939	0.1071037	0.53300716	0.38841969
0.38047875	0.49001666	0.37277126	0.38076953	0.4816118	0.37157806
0.23259421	0.40417869	0.30481694	0.23474284	0.40866067	0.30354094
0.26902968	0.44705303	0.35368354	0.26500556	0.44554015	0.3553064
0.1420849	0.44542467	0.39817535	0.15430503	0.44526867	0.3946804
0.44785005	0.48233625	0.29258582	-0.0004465	0.44697192	0.44771045
			0.44013376	0.47865649	0.29204137
TiO_2 + CO_2			**TiO_2 + Ag + CO_2**		
0.23099863	0.2442563	0.03019416	0.23467446	0.24714347	0.02954312
0.37320052	0.29174237	0.18493959	0.37965391	0.29546886	0.18398403
0.00295174	0.00117003	0.05876288	0.00686862	0.00355091	0.05667662
0.14472105	0.04796304	0.2134246	0.15278946	0.05200032	0.21173978
0.73188225	0.24421325	0.03077678	0.73676764	0.24732031	0.02894799
0.87394893	0.2917441	0.1862467	0.88387636	0.29466465	0.18529383
0.50263795	0.00105136	0.05784652	0.50651636	0.00356664	0.05544038
0.64454626	0.04810173	0.21307129	0.65049662	0.05079913	0.21037185
0.23152206	0.5771719	0.02973817	0.23492155	0.57838494	0.02916704
0.37329467	0.62450324	0.18432594	0.3790916	0.62771201	0.18349149

0.00235488	0.33434088	0.05968921	0.00526576	0.33665614	0.06177886
0.14451682	0.38159388	0.21492919	0.15531264	0.38634844	0.2187376
0.73254231	0.57715471	0.03016988	0.73510704	0.57892712	0.02906266
0.87413652	0.6247656	0.18547188	0.87840042	0.62830402	0.18123621
0.50182995	0.33432499	0.05795351	0.50575885	0.33613997	0.05700092
0.64352707	0.38136124	0.21324249	0.65222393	0.3824227	0.21140139
0.23172104	0.91080073	0.02996184	0.23575118	0.91349641	0.02774563
0.37416175	0.95836124	0.18470745	0.38012627	0.96102507	0.1823904
0.00301081	0.66773943	0.05867558	0.00797885	0.67045883	0.05616514
0.14489272	0.71555037	0.21384067	0.15166485	0.71960186	0.21271099
0.73234982	0.9109121	0.03018977	0.7358978	0.91245182	0.0285475
0.87385198	0.95816671	0.18509462	0.88172293	0.96291911	0.18342387
0.50251331	0.66773963	0.05774113	0.50598228	0.66938975	0.056532
0.64430601	0.71466945	0.21262641	0.65067495	0.72131797	0.21054048
0.04529816	0.18200491	0.06118223	0.04816143	0.18352039	0.05963866
0.19516241	0.23148066	0.22540548	0.20766379	0.23282765	0.2268973
0.32600957	0.2761308	0.09747451	0.3304221	0.27845096	0.09700816
0.48152698	0.32807193	0.2493769	0.49044581	0.33536011	0.2500953
0.18016626	0.06058478	0.01827046	0.18470457	0.06351115	0.01655551
0.33123697	0.11079669	0.18304997	0.33943706	0.11406093	0.18132135
0.39311266	0.29747006	-0.0062616	0.39672805	0.30270405	-0.0070081
0.04990109	0.01549427	0.14596443	0.05723364	0.02091642	0.14426744
0.54479021	0.18181887	0.06023073	0.54701223	0.18350471	0.05735819
0.69461255	0.23154779	0.22517001	0.69828107	0.23229198	0.22397534
0.82591377	0.27591268	0.09848756	0.82569431	0.27927656	0.09758577
0.98192997	0.32823594	0.25082195	0.97518006	0.31952034	0.25387464
0.68099145	0.06079164	0.01831797	0.68615004	0.06300901	0.01722803
0.83196887	0.11099128	0.18384997	0.83649707	0.11279213	0.18069163
0.8945831	0.29780424	-0.0049869	0.89960084	0.30145803	-0.0050441
0.55015179	0.01580715	0.14546271	0.55518502	0.01819743	0.14301242
0.04560877	0.51525828	0.06082157	0.04928491	0.51854503	0.05994941
0.19628767	0.56590298	0.22601685	0.20591961	0.57499842	0.22843042
0.3260889	0.60872049	0.09714896	0.33053516	0.61147387	0.0964484
0.48205409	0.66049097	0.24887937	0.49030305	0.66655412	0.24843509
0.17959971	0.39347079	0.01822818	0.18285261	0.39560279	0.01881436
0.32991694	0.44369394	0.18321238	0.34477072	0.45038925	0.1829457
0.39372362	0.63116562	-0.0065806	0.39703278	0.62989763	-0.0074812
0.04993749	0.35040949	0.14726909	0.05047189	0.35218675	0.14630543
0.54479011	0.51504	0.05951685	0.5502549	0.51771017	0.06072722
0.69507005	0.56527921	0.22504911	0.69816264	0.56896631	0.21916323
0.82634715	0.60791	0.0977379	0.8319858	0.61149118	0.09659325
0.98241565	0.66139926	0.24992424	0.98551532	0.66674385	0.24990519

0.68044411	0.39348014	0.01804108	0.68355237	0.39671115	0.01656652
0.83128609	0.44401615	0.18403017	0.83993956	0.4486948	0.18494661
0.89489148	0.63141003	-0.0058944	0.89759891	0.63305226	-0.0073624
0.54954534	0.35069254	0.14572509	0.55579474	0.34810664	0.14476436
0.04507852	0.8484301	0.06007511	0.04977294	0.85082943	0.05860091
0.19640931	0.89903168	0.22544786	0.20323348	0.90234765	0.22488029
0.32625007	0.94214573	0.09726281	0.3304253	0.94447444	0.09509446
0.48236124	0.99432796	0.24912069	0.48825386	0.99434096	0.24688963
0.18041896	0.72690864	0.01810105	0.18526801	0.72915053	0.01625438
0.33092322	0.77719147	0.1829985	0.33380627	0.77961553	0.18041956
0.39386422	0.96512125	-0.0064287	0.39751057	0.96761795	-0.0088296
0.05011118	0.68428614	0.14631648	0.0563004	0.68696944	0.14546208
0.54479162	0.84833204	0.05938886	0.54775393	0.85002115	0.05651748
0.6952617	0.89821835	0.22486752	0.70382139	0.90331371	0.22447095
0.82603089	0.94250104	0.09780224	0.83060652	0.94249712	0.0960296
0.98236574	0.99360025	0.24956432	0.99002758	0.99901617	0.24806278
0.68136731	0.72708125	0.01826806	0.68466256	0.7281317	0.01653736
0.83123012	0.77712852	0.18311154	0.839126	0.78181983	0.18222379
0.89466694	0.96540776	-0.0057926	0.89811233	0.96687436	-0.0077208
0.54949904	0.68362578	0.14525754	0.55464807	0.69261816	0.143905
0.38762481	0.72018692	0.3658379	0.33959338	0.72407803	0.36074812
0.35722813	0.50514765	0.35575188	0.3590106	0.52354566	0.35969781
0.37309503	0.61292564	0.36036642	0.75963165	0.41736217	0.40871756
			0.90641648	0.34449316	0.33727611
			0.59235858	0.46099504	0.33083795
			0.8593628	0.5708843	0.321694
$TiO_2 + Li_2CO_3$			**$TiO_2 + Ag + Li_2CO_3$**		
0.23091479	0.24270363	0.03262015	0.23232754	0.24583207	0.03504497
0.36893448	0.29164174	0.18879719	0.37799883	0.29661873	0.19101625
0.00132067	0.00108447	0.06047859	-0.0019708	0.00236503	0.05827466
0.14287947	0.04764497	0.21722467	0.14566008	0.05121757	0.21421541
0.73053095	0.24347463	0.03071811	0.72553303	0.24339859	0.03246737
0.86936679	0.28934337	0.18589854	0.86616445	0.2879551	0.18519149
0.50143642	0.00145266	0.06150726	0.49936009	0.00161085	0.06227436
0.64360013	0.04681298	0.21565079	0.64527097	0.04269545	0.21657908
0.23166258	0.57752138	0.02847152	0.22645928	0.57624869	0.02986056
0.37142396	0.62293662	0.18299212	0.36694952	0.62721622	0.18225963
0.00138147	0.33427987	0.05915754	-0.0022393	0.33292398	0.05836646
0.13885353	0.38014678	0.21533584	0.13856035	0.38200715	0.21483183
0.73000937	0.57622367	0.03111243	0.72618753	0.57532621	0.02803936
0.87255504	0.62241453	0.18572837	0.86733951	0.62251267	0.18202369
0.50128924	0.33312254	0.06141155	0.50122847	0.33523997	0.06834368

0.64229969	0.38104478	0.21619841	0.64854156	0.38476392	0.22825151
0.23023004	0.91134963	0.03298353	0.22835693	0.91225762	0.03373436
0.36939768	0.95480922	0.1885072	0.37261597	0.95790146	0.18868617
0.00133326	0.6670215	0.05931356	-0.0030757	0.66684079	0.05727408
0.14051233	0.71184947	0.21554794	0.13523429	0.71576834	0.21222971
0.73057827	0.91047061	0.03182567	0.72749791	0.91173846	0.03089892
0.87472227	0.95865779	0.18640083	0.87605363	0.95851292	0.18594287
0.50136973	0.66752634	0.0584972	0.49904305	0.66734701	0.05783646
0.64791942	0.71608907	0.2117198	0.64532152	0.71771964	0.2108781
0.04421597	0.18172439	0.06249382	0.04196197	0.18267609	0.06297481
0.19142811	0.23059354	0.22945329	0.19004857	0.233099	0.22634904
0.32462394	0.26929246	0.10053405	0.32074057	0.27765194	0.10449653
0.48178266	0.34986661	0.25458693	0.47109191	0.34704175	0.2604817
0.17824717	0.05960253	0.01961675	0.17894306	0.06230604	0.02130229
0.33509153	0.11186323	0.19289672	0.34075334	0.11527764	0.19361179
0.39371962	0.29650546	-0.0030941	0.39491877	0.29595021	0.00155235
0.0515991	0.01890202	0.14857809	0.05113615	0.0167726	0.14677145
0.54608265	0.18221413	0.06300841	0.5443137	0.18212738	0.06710259
0.68817883	0.22865443	0.22776378	0.69509989	0.22050188	0.23221521
0.82464126	0.27598553	0.09813338	0.8232563	0.27689778	0.09961106
0.97478571	0.32372257	0.25061916	0.97614614	0.32312125	0.25332457
0.67888911	0.0596497	0.02017937	0.67409328	0.06046075	0.01994695
0.82650258	0.10879595	0.18380006	0.82758276	0.10741948	0.18279432
0.89318586	0.29610049	-0.0053453	0.88728748	0.29424825	0.995216
0.5461645	0.01735885	0.1494808	0.54751204	0.01443845	0.14998874
0.04430455	0.51482302	0.059212	0.03956008	0.5135712	0.05846209
0.19099657	0.56265208	0.2275481	0.18860912	0.56644503	0.22531046
0.32429811	0.60897816	0.09563782	0.32031312	0.60355902	0.09776196
0.49307943	0.66492128	0.25317172	0.47644183	0.67074289	0.24888297
0.18041003	0.39212337	0.01935133	0.17738968	0.39228255	0.01911739
0.32136971	0.43560812	0.18381543	0.33001945	0.44868042	0.19154519
0.39477461	0.63187402	-0.007048	0.38905586	0.6321875	0.99387814
0.04493838	0.34970159	0.14742014	0.04438229	0.35147937	0.14810832
0.54367589	0.51401863	0.06189657	0.54192846	0.51573574	0.06126953
0.69496959	0.56549952	0.22669027	0.68840026	0.57772188	0.23234392
0.82460089	0.60637401	0.09848211	0.82088282	0.60302198	0.09469407
0.97696122	0.65641012	0.25078543	0.98388145	0.67219918	0.25473334
0.67846209	0.39282058	0.01926472	0.67449529	0.39077404	0.02133008
0.82519786	0.44066361	0.18453713	0.82794585	0.43902323	0.18999718
0.89262478	0.63186624	-0.005024	0.88893776	0.63080202	0.99214284
0.54577111	0.34606689	0.14986429	0.5444288	0.35139646	0.15313839
0.04334511	0.84812535	0.06268611	0.03787145	0.84813506	0.05867598

0.1907264	0.89665862	0.22863117	0.19507599	0.90047253	0.22682886
0.32434878	0.94660702	0.10087792	0.32253317	0.94750975	0.10184546
0.48306666	0.97361579	0.25414498	0.48157814	0.96924385	0.25463639
0.1797911	0.72863384	0.01946766	0.17894489	0.7285353	0.02013612
0.32396554	0.77889031	0.18526408	0.32460615	0.77741779	0.18288254
0.3932849	0.96569744	-0.0027714	0.39084691	0.9667967	0.99796348
0.04772443	0.67937166	0.14729626	0.05021996	0.68597694	0.14332078
0.54361818	0.84849359	0.06188626	0.54121825	0.84854681	0.06211369
0.69679386	0.8982261	0.22728433	0.70200066	0.89888594	0.23201266
0.82536704	0.94185874	0.09941025	0.82367048	0.94553077	0.09785666
0.97899135	0.99452213	0.25174761	0.98420454	0.99396281	0.25078922
0.67966327	0.72679187	0.01910302	0.67613284	0.72796756	0.01806225
0.83503155	0.77819029	0.18369523	0.8253249	0.78037043	0.17824261
0.89330084	0.96577047	-0.0040584	0.88930916	0.96883952	0.99408409
0.55353098	0.68497404	0.14507099	0.54325991	0.6832542	0.14491103
0.45694514	0.56126863	0.37051126	0.49431201	0.53237784	0.36208197
0.46842026	0.6668313	0.44908895	0.61207078	0.68288727	0.42461122
0.46278413	0.76208569	0.36917513	0.46860894	0.72107213	0.36715907
0.46266052	0.66340573	0.39557453	0.52525903	0.64642385	0.38463773
0.47923946	0.50995852	0.29954575	0.45014384	0.50802265	0.28708451
0.48198559	0.81604749	0.29670909	0.47012894	0.80513588	0.3015716
			0.87217906	0.59028261	0.32848994
			0.83303785	0.34419371	0.32370565
			0.75334596	0.59099609	0.42925502
			0.62681943	0.4157006	0.35376516
TiO_2 + C					
0.23104246	0.24329799	0.02277999			
0.35775394	0.28516409	0.17468631			
0.0054445	0.0019964	0.05836336			
0.14445645	0.04616736	0.21584976			
0.73374817	0.24396316	0.03050963			
0.87381222	0.29142078	0.18640271			
0.50434531	0.0007468	0.05948641			
0.64790778	0.04834998	0.2134802			
0.23259497	0.57670036	0.0301466			
0.37561442	0.62528725	0.18546919			
0.00426618	0.33396208	0.05917713			
0.14396757	0.38151387	0.21575292			
0.73357884	0.57745835	0.02926707			
0.87245236	0.62399412	0.18558188			
0.50285942	0.33376289	0.05535677			
0.64227414	0.38083991	0.21087995			

0.23378653	0.91105392	0.03053504			
0.37607471	0.95718179	0.18635954			
0.00340939	0.66767573	0.05899338			
0.14396665	0.71385596	0.21307658			
0.7339131	0.91047445	0.03046888			
0.87646665	0.95877951	0.18469816			
0.50343464	0.66744023	0.058477			
0.64762911	0.7170085	0.21256462			
0.0486627	0.18246466	0.05884617			
0.19366733	0.23040336	0.2270929			
0.32275213	0.2735992	0.09097573			
0.45041132	0.31666235	0.32859071			
0.18074606	0.05874917	0.0151222			
0.33737138	0.11217986	0.19060106			
0.39588409	0.2973586	-0.0106484			
0.05514781	0.01927905	0.14695965			
0.54553115	0.18158229	0.05860578			
0.69786625	0.22774539	0.22677849			
0.82820648	0.27595584	0.09807415			
0.9818031	0.32884289	0.25140405			
0.68267388	0.06002739	0.01912623			
0.83407239	0.11086185	0.18249385			
0.89594847	0.29731678	-0.0054216			
0.55089281	0.01733973	0.14626973			
0.04631513	0.51453846	0.06080743			
0.1961408	0.565906	0.22582739			
0.32649994	0.60098863	0.09785524			
0.48476194	0.6663969	0.24936404			
0.17970554	0.39387185	0.01526121			
0.33634902	0.44436855	0.19022052			
0.39478926	0.63498039	-0.0058783			
0.05270956	0.34888869	0.14745726			
0.54468624	0.51398928	0.05733419			
0.69746496	0.57091527	0.22638514			
0.82555522	0.60678164	0.09714613			
0.98213625	0.6607475	0.24968465			
0.68261766	0.39343064	0.01719093			
0.83232846	0.44379301	0.18317468			
0.89654748	0.63237818	-0.0061341			
0.54057361	0.34721782	0.14351367			
0.0469527	0.849123	0.06073399			
0.19682873	0.8968659	0.22638232			

0.32711519	0.94881141	0.09845655			
0.48518282	0.98967013	0.25027316			
0.18198423	0.72699443	0.01967323			
0.33015608	0.77620553	0.18156053			
0.39619757	0.96075117	-0.0051431			
0.04911052	0.68305948	0.14585362			
0.54694731	0.84821732	0.06133036			
0.70074416	0.89998936	0.2257033			
0.82995046	0.94376514	0.09761075			
0.98179251	0.99120377	0.25061837			
0.68193297	0.72729242	0.01825663			
0.83313117	0.77842624	0.1810819			
0.89590958	0.96445675	-0.0058738			
0.55012819	0.68157197	0.14539553			
0.50984796	0.33658937	0.28782267			

References

[1] K. Awazu, M. Fujimaki, C. Rockstuhl, J. Tominaga, H. Murakami, Y. Ohki, N. Yoshida, T. Watanabe, *J. Am. Chem. Soc.* **2008**, *130*, 1676-1680.
[2] a) G. Kresse, J. Furthmuller, *Phys. Rev. B* **1996**, *54*, 11169-11186; b) J. P. Perdew, K. Burke, M. Ernzerhof, *Phys. Rev. Lett.* **1996**, *77*, 3865-3868.
[3] P. E. Blochl, *Phys. Rev. B* **1994**, *50*, 17953-17979.
[4] X. X. Wang, D. H. Guan, F. Li, M. L. Li, L. J. Zheng, J. J. Xu, *Small* **2021**, *17*, 2100642.
[5] A. Jena, H. C. Hsieh, S. Thoka, S. F. Hu, H. Chang, R. S. Liu, *Chemsuschem* **2020**, *13*, 2719-2725.
[6] D. H. Guan, X. X. Wang, M. L. Li, F. Li, L. J. Zheng, X. L. Huang, J. J. Xu, *Angew. Chem. Int. Ed.* **2020**, *59*, 19518-19524.
[7] Z. Li, M. Li, X. Wang, D. Guan, W. Liu, J. Xu, *J. Mater. Chem. A* **2020**, *8*, 14799-14806.
[8] C. Hu, L. Gong, Y. Xiao, Y. Yuan, N. M. Bedford, Z. Xia, L. Ma, T. Wu, Y. Lin, J. W. Connell, R. Shahbazian-Yassar, J. Lu, K. Amine, L. Dai, *Adv. Mater.* **2020**, *32*, 1907436.
[9] S. Huang, D. Chen, C. Meng, S. Wang, S. Ren, D. Han, M. Xiao, L. Sun, Y. Meng, *Small* **2019**, *15*, 1904830.
[10] C. Wang, Q. Zhang, X. Zhang, X. G. Wang, Z. Xie, Z. Zhou, *Small* **2018**, *14*, 1800641.
[11] Z. Zhang, X. G. Wang, X. Zhang, Z. Xie, Y. N. Chen, L. Ma, Z. Peng, Z. Zhou, *Adv. Sci.* **2018**, *5*, 1700567.
[12] Z. Zhang, Q. Zhang, Y. A. Chen, J. Bao, X. L. Zhou, Z. J. Xie, J. P. Wei, Z. Zhou, *Angew. Chem. Int. Ed.* **2015**, *54*, 6550-6553.

Author Contributions

K. Zhang and J. Li conceived the idea, designed the experiments, analyzed the data, co-wrote and modified the paper. H. Peng and B. Wang directed the project. W. Zhai, X. Kang, C. Wang, and T. Kong helped with materials preparation and characterizations. Z. Zhu, C. Li, M. Liao, L. Ye, Y. Zhao, P. Chen, and Y. Gao provided helpful advice on the working mechanism analyses. All authors discussed the results and commented on the manuscript.